

NESTED COORDINATE BETHE WAVEFUNCTIONS FROM THE BETHE/GAUGE CORRESPONDENCE

OMAR FODA AND MASAHIDE MANABE

To Professor Tetsuji Miwa on his 70th birthday

ABSTRACT. In [1, 2], Nekrasov applied the Bethe/Gauge correspondence to derive the $\mathfrak{su}(2)$ XXX spin-chain coordinate Bethe wavefunction from the IR limit of a 2D $\mathcal{N} = (2, 2)$ supersymmetric A_1 quiver gauge theory with an orbifold-type codimension-2 defect. Later, Bullimore, Kim and Lukowski implemented Nekrasov's construction at the level of the UV A_1 quiver gauge theory, recovered his result, and obtained further extensions of the Bethe/Gauge correspondence [3]. In this work, we extend the construction of the defect to A_M quiver gauge theories to obtain the $\mathfrak{su}(M+1)$ XXX spin-chain nested coordinate Bethe wavefunctions. The extension to XXZ spin-chain is straightforward. Further, we apply a Higgsing procedure to obtain more general A_M quivers and the corresponding wavefunctions, and interpret this procedure (and the Hanany-Witten moves that it involves) on the spin-chain side in terms of Izergin-Korepin-type specializations (and re-assignments) of the parameters of the coordinate Bethe wavefunctions.

1. INTRODUCTION

In [4, 5], Nekrasov and Shatashvili proposed the Bethe/Gauge correspondence between the on-shell Bethe eigenstates of XXX (resp. XXZ) spin-chain Hamiltonians and the vacuum states of 2D $\mathcal{N} = (2, 2)$ supersymmetric (resp. 3D $\mathcal{N} = 2$) quiver gauge theories ¹.

In [1, 2], Nekrasov introduced an orbifold-type codimension-2 defect in the IR limit of an A_1 quiver gauge theory on the gauge side of the correspondence, and obtained the coordinate Bethe wavefunction in the $\mathfrak{su}(2)$ XXX spin- $\frac{1}{2}$ chain on the Bethe side [6, 7] ².

In [3], Bullimore, Kim and Lukowski implemented Nekrasov's defect construction at the level of the UV A-twisted $\mathcal{N} = (2, 2)$ supersymmetric A_1 quiver gauge theories on S^2 , and used the

Key words and phrases. The Bethe/Gauge correspondence. 2-dimensional gauged linear sigma models. The nested coordinate Bethe wavefunctions. XXX spin-chains.

¹ The on-shell Bethe states (the eigenstates of the spin-chain Hamiltonian) are such that the rapidity variables satisfy the Bethe equations, and the positions of the spin variables are summed over. The off-shell Bethe states are such that the rapidity variables do not satisfy any conditions, and the positions of the spin variables are summed over [6, 7].

² We consider only spin-chains with periodic (possibly twisted) boundary conditions. The rapidity variables of the coordinate Bethe wavefunctions can be free, or can be set to satisfy the Bethe equations to enforce periodicity in the case of periodic boundary conditions. By definition, the positions of the spin variables in a coordinate Bethe wavefunction are fixed.

localization formulae of [8, 9] to recover Nekrasov's result, amongst other results that further extend the Bethe/Gauge correspondence.

In this work, we extend the construction of [3] to A_M quiver gauge theories with orbifold-type codimension-2 defects to obtain $\mathfrak{su}(M+1)$ XXX spin-chain nested coordinate Bethe wavefunctions, with spin states in the fundamental representation.

Further, we apply a Higgsing procedure to obtain more general A_M quiver gauge theories with codimension-2 defects, and their corresponding nested coordinate Bethe wavefunctions, and interpret these generalizations on the spin-chain side (and the Hanany-Witten moves that they involve) as Izergin-Korepin-type specializations (and re-assignments of the roles) of the parameters. While we focus on results in XXX spin-chains, we outline their straightforward extension to XXZ spin-chains.

1.1. Outline of contents. In Section 2, we recall the localization formulae of Closset, Cremonesi and Park, for 2D $\mathcal{N} = (2, 2)$ quiver gauge theories on S^2 [8] (and that of Benini and Zaffaroni, for $\mathcal{N} = 2$ quiver gauge theories on $S^2 \times S^1$ [9]), used in [3] to construct Nekrasov's orbifold defect in 2D A_1 quiver gauge theory. Generalizing the discussion in [3] for A_1 quiver gauge theory, we formally introduce the equivariant characters and reconstruct the localization formulae in [8, 9] from them.

In Section 3, we recall the Bethe/Gauge correspondence [4, 5] for A_M linear quiver gauge theories, and provide the equivariant characters for them.

In Section 4, after briefly recalling the construction of orbifold defects in A_1 quiver gauge theory, we extend this construction to a simple A_M linear quiver gauge theory and obtain the nested coordinate Bethe wavefunctions of the $\mathfrak{su}(M+1)$ XXX spin-chain with spin states in the fundamental representation.

In Section 5, using a Higgsing procedure, we generalize the orbifold construction of Section 4 to more general A_M linear quiver gauge theories and find the corresponding partition functions (as specializations of coordinate Bethe wavefunctions) of the corresponding $\mathfrak{su}(M+1)$ vertex lattice models. In Section 6, we interpret the Higgsing procedure as an Izergin-Korepin-type specialization of the lattice parameters on the Bethe side of the Bethe/Gauge correspondence, and interpret the Hanany-Witten moves that are involved in the Higgsing on the gauge side as a re-assignment of the lattice parameters on the Bethe side, and in Section 7, we include remarks.

In Appendix A, we discuss the partial domain wall partition functions (DWPFs) in the rational $\mathfrak{su}(2)$ (six-)vertex model and prove Proposition 4.5, and in Appendix B, we define the partition function of the $\mathfrak{su}(M+1)$ vertex model which corresponds to the orbifold defect in the A_M quiver constructed in the present work.

2. REWRITING THE LOCALIZATION FORMULAE

We review the localization formulae of the partition functions of the A -twisted gauged linear sigma models (GLSMs) [10, 11], which are 2D A -twisted $\mathcal{N} = (2, 2)$ supersymmetric gauge theories on the Ω -deformed S^2_{\hbar} [8] (and 3D twisted $\mathcal{N} = 2$ gauge theories on $S^2_{\hbar} \times S^1$ [9]), where \hbar is the Ω -deformation parameter. Following [3], we provide the localization formulae in terms of equivariant characters which are more fundamental objects than the partition functions. The equivariant characters are used to construct orbifold defects in Sections 4 and 5.³

2.1. Equivariant characters. Consider the 2D $\mathcal{N} = (2, 2)$ (or 3D $\mathcal{N} = 2$) supersymmetric gauge theory consisting of a vector multiplet V in a Lie algebra \mathfrak{g} , of gauge group G , and L chiral matter multiplets $\Phi_{\mathfrak{R}_i}^{r_i}$, with representations \mathfrak{R}_i of \mathfrak{g} , $U(1)$ vector R -charges r_i and twisted masses λ_i , $i = 1, \dots, L$. In the present work, $r_i = 0$ or 2 . The vector multiplet V contains scalars $\mathbf{u} = \{u_1, \dots, u_{\text{rk}(\mathfrak{g})}\}$, which take values in $\mathfrak{h} \otimes_{\mathbb{R}} \mathbb{C}$ and parametrize the Coulomb branch of the gauge theory, where $\text{rk}(\mathfrak{g})$ is the rank of \mathfrak{g} and \mathfrak{h} is the Cartan subalgebra of \mathfrak{g} .

Definition 2.1. *The equivariant characters of the vector multiplet V and the chiral matter multiplet $\Phi_{\mathfrak{R}}^r$ are*

$$(2.1) \quad \chi_{\hbar}^V(\mathbf{u}) := - \sum_{\alpha \in \Delta_+} \frac{e^{\alpha(\mathbf{u})} + e^{-\alpha(\mathbf{u})}}{1 - e^{\hbar\alpha}}, \quad \chi_{\hbar}^{\Phi_{\mathfrak{R}}^r}(\mathbf{u}) := \sum_{\rho \in \mathfrak{R}} \frac{e^{\rho(\mathbf{u}) + \lambda + \hbar\delta_{r,2}}}{1 - e^{\hbar\rho}},$$

where Δ_+ is the set of positive roots of \mathfrak{g} , while $\alpha(\mathbf{u})$ and $\rho(\mathbf{u})$ are the canonical pairings. The equivariant characters charged with GNO charges $\mathbf{d} = \{d_1, \dots, d_{\text{rk}(\mathfrak{g})}\}$, $d_a \in \pi_1(U(1)) \cong \mathbb{Z}$, associated with the quantized magnetic fluxes of the $U(1)^{\text{rk}(\mathfrak{g})}$ gauge fields on S^2_{\hbar} , are

$$(2.2) \quad \chi_{\hbar, \mathbf{d}}^P(\mathbf{u}) := \chi_{+\hbar}^P(\mathbf{u}|_+) + \chi_{-\hbar}^P(\mathbf{u}|_-),$$

where $P = V$ or $\Phi_{\mathfrak{R}}^r$, and

$$(2.3) \quad u_a|_{\pm} = u_a \mp \frac{d_a}{2} \hbar$$

where the characters $\chi_{+\hbar}^P(\mathbf{u}|_+)$ and $\chi_{-\hbar}^P(\mathbf{u}|_-)$ are defined on the north pole and the south pole of S^2_{\hbar} , respectively.

Definition 2.2. *The total equivariant character is*

$$(2.4) \quad \chi_{\hbar}^{\text{total}}(\mathbf{u}) := \chi_{\hbar}^V(\mathbf{u}) + \sum_{i=1}^L \chi_{\hbar}^{\Phi_{\mathfrak{R}_i}^{r_i}}(\mathbf{u}),$$

³ In the present work, we use ‘equivariant character’, as well as the notation \hbar for the Ω -deformation parameter, and γ for a twisted mass parameter. In [3], Bullimore *et al.* use ‘equivariant index’ instead of ‘equivariant character’, as well as the notation ϵ for the Ω -deformation parameter, and \hbar for the twisted mass parameter.

and the total equivariant character with charges \mathbf{d} is

$$(2.5) \quad \chi_{\hbar, \mathbf{d}}^{\text{total}}(\mathbf{u}) := \chi_{+\hbar}^{\text{total}}(\mathbf{u}|_+) + \chi_{-\hbar}^{\text{total}}(\mathbf{u}|_-) = \chi_{\hbar, \mathbf{d}}^V(\mathbf{u}) + \sum_{i=1}^L \chi_{\hbar, \mathbf{d}}^{\Phi_{\mathfrak{R}^i}^{r_i}}(\mathbf{u})$$

2.2. Partition functions. Each character $\chi_{\hbar, \mathbf{d}}^P(\mathbf{u})$ with charges \mathbf{d} can be expanded as

$$(2.6) \quad \chi_{\hbar, \mathbf{d}}^P(\mathbf{u}) = \sum_I e^{w_I(\mathbf{u}; \mathbf{d}; \hbar)} - \sum_J e^{v_J(\mathbf{u}; \mathbf{d}; \hbar)},$$

where (2.6) defines w_I and v_J , and we obtain the building blocks of the topologically twisted partition functions of 2D and 3D gauge theories by

$$(2.7) \quad \widehat{\mathcal{Z}}_{\mathbf{d}}^P(\mathbf{u}; \hbar) = \frac{\prod_J v_J(\mathbf{u}; \mathbf{d}; \hbar)}{\prod_I w_I(\mathbf{u}; \mathbf{d}; \hbar)},$$

and

$$(2.8) \quad \widehat{\mathcal{Z}}_{\mathbf{d}}^{K, P}(\mathbf{u}; \hbar) = \frac{\prod_J 2 \sinh \left(v_J(\mathbf{u}; \mathbf{d}; \hbar)/2 \right)}{\prod_I 2 \sinh \left(w_I(\mathbf{u}; \mathbf{d}; \hbar)/2 \right)},$$

respectively.

Proposition 2.3. *The partition functions (2.7) and (2.8), which are obtained from Definition 2.1, as*

$$(2.9) \quad \begin{aligned} \widehat{\mathcal{Z}}_{\mathbf{d}}^V(\mathbf{u}; \hbar) &= (-1)^{\sum_{\alpha \in \Delta_+} (\alpha(\mathbf{d})+1)} \prod_{\alpha \in \Delta_+} \left(\alpha(\mathbf{u})^2 - \frac{\alpha(\mathbf{d})^2}{4} \hbar^2 \right), \\ \widehat{\mathcal{Z}}_{\mathbf{d}}^{\Phi_{\mathfrak{R}^r}^r}(\mathbf{u}; \hbar) &= \prod_{\rho \in \mathfrak{R}} \frac{\hbar^{r-\rho(\mathbf{d})-1}}{\left(\frac{\rho(\mathbf{u})+\lambda}{\hbar} + \frac{r-\rho(\mathbf{d})}{2} \right)_{\rho(\mathbf{d})+1-r}}, \end{aligned}$$

and

$$(2.10) \quad \begin{aligned} \widehat{\mathcal{Z}}_{\mathbf{d}}^{K, V}(\mathbf{u}; \hbar) &= \left(-q^{-\frac{1}{2}} \right)^{\sum_{\alpha \in \Delta_+} \alpha(\mathbf{d})} \prod_{\alpha \in \Delta_+} \left(1 - \mathbf{u}^{-\alpha} q^{\frac{1}{2}\alpha(\mathbf{d})} \right) \left(1 - \mathbf{u}^{\alpha} q^{\frac{1}{2}\alpha(\mathbf{d})} \right), \\ \widehat{\mathcal{Z}}_{\mathbf{d}}^{K, \Phi_{\mathfrak{R}^r}^r}(\mathbf{u}; \hbar) &= \prod_{\rho \in \mathfrak{R}} \frac{\left(\mathbf{u}^{\rho} \Lambda \right)^{\frac{\rho(\mathbf{d})+1-r}{2}}}{\left(\mathbf{u}^{\rho} \Lambda q^{\frac{r-\rho(\mathbf{d})}{2}}; q \right)_{\rho(\mathbf{d})+1-r}}, \end{aligned}$$

respectively, give the building blocks of 2D and 3D topologically twisted partition functions in [8, 9] (see Proposition 2.4). Here $U_a = e^{-u_a}$, $\Lambda = e^{-\lambda}$, $q = e^{-\hbar}$, $\mathbf{u}^{\alpha} = e^{-\alpha(\mathbf{u})}$, and $\mathbf{u}^{\rho} = e^{-\rho(\mathbf{u})}$.

In the above proposition, the Pochhammer and q -Pochhammer symbols are, respectively, defined by

$$(2.11) \quad (x)_d = \frac{\Gamma(x+d)}{\Gamma(x)} = \begin{cases} \prod_{\ell=0}^{d-1} (x+\ell) & \text{if } d > 0, \\ 1 & \text{if } d = 0, \\ \left(\prod_{\ell=d}^{-1} (x+\ell) \right)^{-1} & \text{if } d < 0, \end{cases}$$

and

$$(2.12) \quad (x; q)_d = \begin{cases} \prod_{\ell=0}^d (1 - xq^\ell) & \text{if } d > 0, \\ 1 & \text{if } d = 0, \\ \prod_{\ell=d}^{-1} (1 - xq^\ell)^{-1} & \text{if } d < 0 \end{cases}$$

In the following, we assume that the gauge group G contains central $U(1)^c$ factors, and then one can deform the gauge theory by the associated Fayet-Iliopoulos (FI) parameters ξ^a , and theta angles θ^a , $a = 1, \dots, c$.

Proposition 2.4 ([8, 9]). *Combining the complexified FI parameters $\tau^a = i\xi^a + \frac{1}{2\pi}\theta^a$ with the building blocks in Proposition 2.3 obtained from (2.5), up to sign factors, the partition function of the A-twisted GLSM on S_h^2 is given by*

$$(2.13) \quad Z_{S_h^2} = \frac{1}{|\mathcal{W}|} \sum_{\mathbf{d} \in \mathbb{Z}^{\text{rk}(\mathfrak{g})}} \oint_{\Gamma} d^{\text{rk}(\mathfrak{g})} u \widehat{\mathcal{Z}}_{\mathbf{d}}^{\text{total}}(\mathbf{u}; \hbar),$$

where

$$(2.14) \quad \widehat{\mathcal{Z}}_{\mathbf{d}}^{\text{total}}(\mathbf{u}; \hbar) := e^{2\pi i \tau(\mathbf{d})} \widehat{\mathcal{Z}}_{\mathbf{d}}^V(\mathbf{u}; \hbar) \prod_{i=1}^L \widehat{\mathcal{Z}}_{\mathbf{d}}^{\Phi_{\mathfrak{g}_i}^{r_i}}(\mathbf{u}; \hbar)$$

Here $|\mathcal{W}|$ is the order of the Weyl group of G , and the pairing $\tau(\mathbf{d}) = \sum_a \tau^a d_a$ is defined by embedding $\boldsymbol{\tau}$ into $\mathfrak{h}^* \otimes_{\mathbb{R}} \mathbb{C}$. The contour integral along Γ is given by the Jeffrey-Kirwan residue operation (JK contour integral) [12, 13, 14] (see also [15]), which picks relevant poles of the integrand. Similarly, the correlation function of two codimension-2 defects, $\mathcal{O}_N(\mathbf{u})$ and $\mathcal{O}_S(\mathbf{u})$, inserted at the north pole and at the south pole of S_h^2 , respectively, is given by

$$(2.15) \quad \langle \mathcal{O}_N(\mathbf{u}) \mathcal{O}_S(\mathbf{u}) \rangle_{S_h^2} = \frac{1}{|\mathcal{W}|} \sum_{\mathbf{d} \in \mathbb{Z}^{\text{rk}(\mathfrak{g})}} \oint_{\Gamma} d^{\text{rk}(\mathfrak{g})} u \widehat{\mathcal{Z}}_{\mathbf{d}}^{\text{total}}(\mathbf{u}; \hbar) \mathcal{O}_N(\mathbf{u}|_+) \mathcal{O}_S(\mathbf{u}|_-)$$

The topologically twisted partition function and correlation functions of the $\mathcal{N} = 2$ gauge theory on $S_h^2 \times S^1$ are obtained, up to Chern-Simons factors, by replacing $\widehat{\mathcal{Z}}_{\mathbf{d}}^P(\mathbf{u}; \hbar)$ with $\widehat{\mathcal{Z}}_{\mathbf{d}}^{\text{K},P}(\mathbf{u}; \hbar)$ in the above formulae.

3. THE BETHE/GAUGE CORRESPONDENCE

We recall the basics of the Bethe/Gauge correspondence [4, 5], between the supersymmetric vacua of $2D \mathcal{N} = (2, 2)$ (resp. $3D \mathcal{N} = 2$) A_M linear quiver gauge theories as in Figure 1, and the Bethe eigenfunctions of XXX (resp. XXZ) spin-chain Hamiltonians, with spins in the fundamental representation of $\mathfrak{su}(M+1)$.

The A_M quiver gauge theory which corresponds to the $\mathfrak{su}(M+1)$ XXX spin-chain, with spins in the fundamental representation, is described by an A-twisted GLSM, on the Ω -deformed S_h^2 ,

| | 2D/3D gauge with A_M quiver (Figure 1) | $\mathfrak{su}(M+1)$ XXX/XXZ spin-chain |
|------------------|--|--|
| $u_a^{(p)}$ | vector multiplet scalar | Bethe root |
| $m_i^{(p)}$ | twisted mass | inhomogeneity |
| γ | twisted mass | coupling constant |
| \mathfrak{q}_p | exponentiated FI parameter | periodic spin-chain boundary twist parameter |
| (3.7) | effective twisted superpotential | Yang-Yang function |
| (3.8) | vacuum equation | nested Bethe equation |

TABLE 2. The Bethe/Gauge dictionary, where $a = 1, \dots, k_p$, $i = 1, \dots, L_p$, $p = 1, \dots, M$. Here k_p is the number of vector multiplet scalars in $U(k_p)$ on the gauge side/spin excitations on the Bethe side, and L_p is the number of (anti-)fundamental flavors in $U(k_p)$ on the gauge side/total number of spins on the Bethe side.

for the $U(k_p)$ vector multiplets $V^{(p)}$ and the chiral matter multiplets in Table 1 as

$$\begin{aligned}
\chi_{\hbar}^{V^{(p)}}(\mathbf{u}_{k_p}^{(p)}) &= -\sum_{a \neq b}^{k_p} \frac{e^{u_{a,b}^{(p)}}}{1 - e^{\hbar}}, & \chi_{\hbar}^{\Phi^{(p)}}(\mathbf{u}_{k_p}^{(p)}) &= \sum_{a,b=1}^{k_p} \frac{e^{u_{a,b}^{(p)} + \gamma + \hbar}}{1 - e^{\hbar}}, \\
\chi_{\hbar}^{X_i^{(p)}}(\mathbf{u}_{k_p}^{(p)}) &= \sum_{a=1}^{k_p} \frac{e^{u_a^{(p)} - m_i^{(p)} - \frac{\gamma}{2}}}{1 - e^{\hbar}}, & \chi_{\hbar}^{Y_i^{(p)}}(\mathbf{u}_{k_p}^{(p)}) &= \sum_{a=1}^{k_p} \frac{e^{-u_a^{(p)} + m_i^{(p)} - \frac{\gamma}{2}}}{1 - e^{\hbar}}, \\
\chi_{\hbar}^{A^{(p)}}(\mathbf{u}_{k_p}^{(p)}, \mathbf{u}_{k_{p+1}}^{(p+1)}) &= \sum_{a=1}^{k_p} \sum_{b=1}^{k_{p+1}} \frac{e^{u_a^{(p)} - u_b^{(p+1)} - \frac{\gamma}{2}}}{1 - e^{\hbar}}, \\
\chi_{\hbar}^{B^{(p)}}(\mathbf{u}_{k_p}^{(p)}, \mathbf{u}_{k_{p+1}}^{(p+1)}) &= \sum_{a=1}^{k_p} \sum_{b=1}^{k_{p+1}} \frac{e^{-u_a^{(p)} + u_b^{(p+1)} - \frac{\gamma}{2}}}{1 - e^{\hbar}},
\end{aligned}
\tag{3.1}$$

where $u_{a,b}^{(p)} = u_a^{(p)} - u_b^{(p)}$. Then, the building blocks of the S^2 partition function in Proposition

2.3 are obtained as

$$\begin{aligned}
\widehat{\mathcal{Z}}_{\mathbf{d}_{k_p}^{(p)}}^{V^{(p)}}(\mathbf{u}_{k_p}^{(p)}; \hbar) &= (-1)^{(k_p-1)\sum_{a=1}^{k_p} (d_a^{(p)} + \frac{1}{2})} \prod_{a < b}^{k_p} \left((u_{a,b}^{(p)})^2 - \frac{(d_{a,b}^{(p)})^2}{4} \hbar^2 \right), \\
\widehat{\mathcal{Z}}_{\mathbf{d}_{k_p}^{(p)}}^{\Phi^{(p)}}(\mathbf{u}_{k_p}^{(p)}; \hbar) &= \prod_{a,b=1}^{k_p} \mathcal{Z}^{(d_{a,b}^{(p)}-2)} \left(u_{a,b}^{(p)} + \gamma \right), \\
\widehat{\mathcal{Z}}_{\mathbf{d}_{k_p}^{(p)}}^{X_i^{(p)}}(\mathbf{u}_{k_p}^{(p)}; \hbar) &= \prod_{a=1}^{k_p} \mathcal{Z}^{(d_a^{(p)})} \left(u_a^{(p)} - m_i^{(p)} - \frac{\gamma}{2} \right), \\
\widehat{\mathcal{Z}}_{\mathbf{d}_{k_p}^{(p)}}^{Y_i^{(p)}}(\mathbf{u}_{k_p}^{(p)}; \hbar) &= \prod_{a=1}^{k_p} \mathcal{Z}^{(-d_a^{(p)})} \left(-u_a^{(p)} + m_i^{(p)} - \frac{\gamma}{2} \right), \\
\widehat{\mathcal{Z}}_{\mathbf{d}_{k_p}^{(p)}, \mathbf{d}_{k_{p+1}}^{(p+1)}}^{A^{(p)}}(\mathbf{u}_{k_p}^{(p)}, \mathbf{u}_{k_{p+1}}^{(p+1)}; \hbar) &= \prod_{a=1}^{k_p} \prod_{b=1}^{k_{p+1}} \mathcal{Z}^{(d_a^{(p)} - d_b^{(p+1)})} \left(u_a^{(p)} - u_b^{(p+1)} - \frac{\gamma}{2} \right), \\
\widehat{\mathcal{Z}}_{\mathbf{d}_{k_p}^{(p)}, \mathbf{d}_{k_{p+1}}^{(p+1)}}^{B^{(p)}}(\mathbf{u}_{k_p}^{(p)}, \mathbf{u}_{k_{p+1}}^{(p+1)}; \hbar) &= \prod_{a=1}^{k_p} \prod_{b=1}^{k_{p+1}} \mathcal{Z}^{(-d_a^{(p)} + d_b^{(p+1)})} \left(-u_a^{(p)} + u_b^{(p+1)} - \frac{\gamma}{2} \right),
\end{aligned}
\tag{3.2}$$

where $\mathbf{d}_{\mathbf{k}}^M = \{\mathbf{d}_{k_1}^{(1)}, \dots, \mathbf{d}_{k_M}^{(M)}\}$ with $\mathbf{d}_{k_p}^{(p)} = \{d_1^{(p)}, \dots, d_{k_p}^{(p)}\}$, $d_a^{(p)} \in \mathbb{Z}$, $p = 1, \dots, M$, are sets of GNO charges, $d_{a,b}^{(p)} = d_a^{(p)} - d_b^{(p)}$, and

$$\mathcal{Z}^{(d)}(u) = \begin{cases} \prod_{\ell=0}^d \left(u - \frac{d}{2} \hbar + \ell \hbar \right)^{-1} & \text{if } d \geq 0, \\ \prod_{\ell=1}^{-d-1} \left(u + \frac{d}{2} \hbar + \ell \hbar \right) & \text{if } d < 0 \end{cases}
\tag{3.3}$$

Combining (3.2) with the complexified FI parameters τ^p , $p = 1, \dots, M$, associated with the central $U(1)^M \subset U(k_1) \times \dots \times U(k_M)$, the integrand (2.14) of the S^2 partition function is

$$\begin{aligned}
\widehat{\mathcal{Z}}_{\mathbf{d}_{\mathbf{k}}^M}^{\text{total}}(\mathbf{u}_{\mathbf{k}}^M; \hbar) &= \\
&\prod_{p=1}^M \mathfrak{q}_p^{\sum_{a=1}^{k_p} d_a^{(p)}} \widehat{\mathcal{Z}}_{\mathbf{d}_{k_p}^{(p)}}^{V^{(p)}}(\mathbf{u}_{k_p}^{(p)}; \hbar) \widehat{\mathcal{Z}}_{\mathbf{d}_{k_p}^{(p)}}^{\Phi^{(p)}}(\mathbf{u}_{k_p}^{(p)}; \hbar) \times \prod_{i=1}^{L_p} \widehat{\mathcal{Z}}_{\mathbf{d}_{k_p}^{(p)}}^{X_i^{(p)}}(\mathbf{u}_{k_p}^{(p)}; \hbar) \widehat{\mathcal{Z}}_{\mathbf{d}_{k_p}^{(p)}}^{Y_i^{(p)}}(\mathbf{u}_{k_p}^{(p)}; \hbar) \\
&\times \prod_{p=1}^{M-1} \widehat{\mathcal{Z}}_{\mathbf{d}_{k_p}^{(p)}, \mathbf{d}_{k_{p+1}}^{(p+1)}}^{A^{(p)}}(\mathbf{u}_{k_p}^{(p)}, \mathbf{u}_{k_{p+1}}^{(p+1)}; \hbar) \widehat{\mathcal{Z}}_{\mathbf{d}_{k_p}^{(p)}, \mathbf{d}_{k_{p+1}}^{(p+1)}}^{B^{(p)}}(\mathbf{u}_{k_p}^{(p)}, \mathbf{u}_{k_{p+1}}^{(p+1)}; \hbar),
\end{aligned}
\tag{3.4}$$

where $\mathfrak{q}_p = (-1)^{L_p + k_{p-1} + k_p} e^{2\pi i \tau^p}$ are exponentiated FI parameters.

In the limit $\hbar \rightarrow 0$, with positive FI parameters $\xi^p > 0$, and summing over the GNO charges $\mathbf{d}_{\mathbf{k}}^M$ with $d_a^{(p)} \geq 0$, the partition function (2.13) can be written in terms of a contour integral around the roots of the vacuum equations [8]

$$Z_{S^2} = \oint_{\Gamma_{\text{eff}}} \prod_{p=1}^M \frac{d^{k_p} u^{(p)}}{k_p!} \frac{(-1)^{\frac{k_p}{2}(k_p-1)}}{\prod_{a=1}^{k_p} \left(1 - e^{2\pi i \partial_{u_a^{(p)}} \mathcal{W}_{\text{eff}}(\mathbf{u}_{\mathbf{k}}^M)} \right)} \times \mathcal{Z}_0(\mathbf{u}_{\mathbf{k}}^M),
\tag{3.5}$$

where

$$(3.6) \quad \mathcal{Z}_0(\mathbf{u}_k^M) = \prod_{p=1}^M \frac{\prod_{a<b}^{k_p} \left(u_{a,b}^{(p)}\right)^2 \cdot \prod_{a,b=1}^{k_p} \left(u_{a,b}^{(p)} + \gamma\right)}{\prod_{i=1}^{L_p} \prod_{a=1}^{k_p} \left(u_a^{(p)} - m_i^{(p)} - \frac{\gamma}{2}\right) \left(-u_a^{(p)} + m_i^{(p)} - \frac{\gamma}{2}\right)} \\ \times \prod_{p=1}^{M-1} \frac{1}{\prod_{a=1}^{k_p} \prod_{b=1}^{k_{p+1}} \left(u_a^{(p)} - u_b^{(p+1)} - \frac{\gamma}{2}\right) \left(-u_a^{(p)} + u_b^{(p+1)} - \frac{\gamma}{2}\right)}$$

Here the effective twisted superpotential [4] (in the denominator of the integrand),

$$(3.7) \quad \mathcal{W}_{\text{eff}}(\mathbf{u}_k^M) = \mathcal{W}_{\text{cl}}(\mathbf{u}_k^M) + \mathcal{W}_{\text{vec}}(\mathbf{u}_k^M) + \mathcal{W}_{\text{matt}}(\mathbf{u}_k^M),$$

consists of

$$\mathcal{W}_{\text{cl}}(\mathbf{u}_k^M) = \sum_{p=1}^M \tau^p \sum_{a=1}^{k_p} u_a^{(p)}, \\ \mathcal{W}_{\text{vec}}(\mathbf{u}_k^M) = -\frac{1}{2} \sum_{p=1}^M \sum_{a<b}^{k_p} u_{a,b}^{(p)} = -\frac{1}{2} \sum_{p=1}^M \sum_{a=1}^{k_p} \left(k_p - 2a + 1\right) u_a^{(p)}, \\ \mathcal{W}_{\text{matt}}(\mathbf{u}_k^M) = -\frac{1}{2\pi i} \left[\sum_{p=1}^M \sum_{i=1}^{L_p} \sum_{a=1}^{k_p} \left(u_a^{(p)} - m_i^{(p)} - \frac{\gamma}{2}\right) \left(\log \left(u_a^{(p)} - m_i^{(p)} - \frac{\gamma}{2}\right) - 1\right) \right. \\ \left. + \sum_{p=1}^M \sum_{i=1}^{L_p} \sum_{a=1}^{k_p} \left(-u_a^{(p)} + m_i^{(p)} - \frac{\gamma}{2}\right) \left(\log \left(-u_a^{(p)} + m_i^{(p)} - \frac{\gamma}{2}\right) - 1\right) \right. \\ \left. + \sum_{p=1}^M \sum_{a,b=1}^{k_p} \left(u_{a,b}^{(p)} + \gamma\right) \left(\log \left(u_{a,b}^{(p)} + \gamma\right) - 1\right) \right. \\ \left. + \sum_{p=1}^{M-1} \sum_{a=1}^{k_p} \sum_{b=1}^{k_{p+1}} \left(u_a^{(p)} - u_b^{(p+1)} - \frac{\gamma}{2}\right) \left(\log \left(u_a^{(p)} - u_b^{(p+1)} - \frac{\gamma}{2}\right) - 1\right) \right. \\ \left. + \sum_{p=1}^{M-1} \sum_{a=1}^{k_p} \sum_{b=1}^{k_{p+1}} \left(-u_a^{(p)} + u_b^{(p+1)} - \frac{\gamma}{2}\right) \left(\log \left(-u_a^{(p)} + u_b^{(p+1)} - \frac{\gamma}{2}\right) - 1\right) \right]$$

The contour Γ_{eff} encloses the roots of vacuum equations $e^{2\pi i \partial_{u_a^{(p)}} \mathcal{W}_{\text{eff}}(\mathbf{u}_k^M)} = 1$,

$$(3.8) \quad \prod_{i=1}^{L_p} \frac{u_a^{(p)} - m_i^{(p)} - \frac{\gamma}{2}}{u_a^{(p)} - m_i^{(p)} + \frac{\gamma}{2}} = \mathfrak{q}_p \prod_{b \neq a}^{k_p} \frac{u_{a,b}^{(p)} - \gamma}{u_{a,b}^{(p)} + \gamma} \times \prod_{b=1}^{k_{p-1}} \frac{u_a^{(p)} - u_b^{(p-1)} + \frac{\gamma}{2}}{u_a^{(p)} - u_b^{(p-1)} - \frac{\gamma}{2}} \times \prod_{b=1}^{k_{p+1}} \frac{u_a^{(p)} - u_b^{(p+1)} + \frac{\gamma}{2}}{u_a^{(p)} - u_b^{(p+1)} - \frac{\gamma}{2}},$$

where $a = 1, \dots, k_p$, $p = 1, \dots, M$, $k_0 = k_{M+1} = 0$. These vacuum equations are the nested Bethe equations of the $\mathfrak{su}(M+1)$ XXX spin-chain (see the Bethe/Gauge dictionary in Table 2), which is the starting point of the Bethe/Gauge correspondence [4, 5].

Remark 3.1. The 3D uplift of the above results for XXZ spin-chains is straightforward [4] (see also [16]).

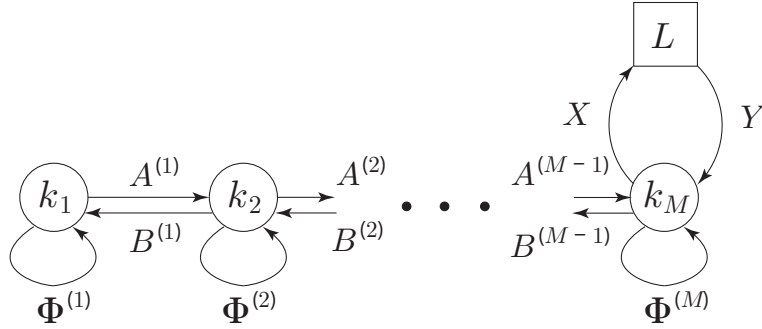


FIGURE 2. The A_M linear quiver that corresponds to Figure 1 with the ranks of the flavour groups $L_i = 0$, $i = 1, \dots, M-1$, $L_M = L$, and the ranks of the gauge groups $k_1 \leq k_2 \leq \dots \leq k_M \leq L$.

| Field | $U(k)$ | twisted mass | $U(1)_R$ |
|--------|--------------------|---------------------------|----------|
| X_i | \mathbf{k} | $-m_i - \frac{\gamma}{2}$ | 0 |
| Y_i | $\bar{\mathbf{k}}$ | $m_i - \frac{\gamma}{2}$ | 0 |
| Φ | \mathbf{adj} | γ | 2 |

TABLE 3. The matter content of the A_1 quiver gauge theory that corresponds to the $\mathfrak{su}(2)$ spin-chain. Here $i = 1, \dots, L$, $k \leq L$.

4. NESTED COORDINATE BETHE WAVEFUNCTIONS FROM ORBIFOLD DEFECTS

We review the construction of orbifold-type codimension-2 defects in the A_1 quiver gauge theory that corresponds to the $\mathfrak{su}(2)$ spin-chain [1, 2, 3], then extend that to the A_M quiver gauge theory that corresponds to the $\mathfrak{su}(M+1)$ spin-chain, described by the A_M quiver in Figure 2.⁴

4.1. Orbifold defect for A_1 quiver. Consider the A-twisted $U(k)$ GLSM on S^2_\hbar , with matter content as in Table 3, and the superpotential $W = \sum_{i=1}^L \sum_{a,b=1}^k X_{i,a} \Phi_{a,b} Y_{b,i}$, $k \leq L$. In this case, the equivariant characters (3.1) are given by

$$(4.1) \quad \begin{aligned} \chi_\hbar^V(\mathbf{u}_k) &= - \sum_{a \neq b}^k \frac{e^{u_{a,b}}}{1 - e^\hbar}, & \chi_\hbar^\Phi(\mathbf{u}_k) &= \sum_{a,b=1}^k \frac{e^{u_{a,b} + \gamma + \hbar}}{1 - e^\hbar}, \\ \chi_\hbar^{X_i}(\mathbf{u}_k) &= \sum_{a=1}^k \frac{e^{u_a - m_i - \frac{\gamma}{2}}}{1 - e^\hbar}, & \chi_\hbar^{Y_i}(\mathbf{u}_k) &= \sum_{a=1}^k \frac{e^{-u_a + m_i - \frac{\gamma}{2}}}{1 - e^\hbar} \end{aligned}$$

Now, we recall the construction of orbifold defects for the A_1 quiver in [1, 2, 3]. The orbifold defects inserted at the north (or south) pole of S^2_\hbar are characterized by a discrete holonomy ω^n ,

⁴ For a suitable choice of the FI parameters, the GLSM described by the A_M quiver in Figure 2 flows in the IR limit to a non-linear sigma model with the cotangent bundle of a partial flag variety as a target. This partial flag variety is defined by the set of subspaces $\{\{0\} \subset \mathbb{C}^{k_1} \subset \mathbb{C}^{k_2} \subset \dots \subset \mathbb{C}^{k_M} \subset \mathbb{C}^L\}$, in \mathbb{C}^L . In the case of $k_p = p$, $M = L - 1$, the variety is called the complete flag variety.

$n = 0, 1, \dots, L-1$, with $\omega^L = 1$, associated with a \mathbb{Z}_L orbifold around the north (or south) pole, such that the gauge symmetry $U(k)$ and the flavor symmetry $U(L)$ are broken to a maximal torus. Firstly, for constructing such orbifold defects, we change the parameters

$$(4.2) \quad m_i \rightarrow m_i + \left(i-1\right) \frac{\hbar}{L}, \quad u_a|_{\pm} \rightarrow u_a|_{\pm} + \left(I_a-1\right) \frac{\hbar}{L}, \quad \hbar \rightarrow \frac{\hbar}{L},$$

in the total equivariant character $\chi_{+\hbar}^{\text{total}}(\mathbf{u}_k|_+)$ or $\chi_{-\hbar}^{\text{total}}(\mathbf{u}_k|_-)$ in (2.5), which is composed of the expressions in (4.1), where

$$(4.3) \quad \mathbf{I}_k = \{I_1, \dots, I_k\} \subset \mathbf{I}_L = \{1, \dots, L\}, \quad I_a < I_{a+1},$$

is an ordered set that characterizes the orbifold defect. Next, taking the \mathbb{Z}_L invariant part under $\hbar \rightarrow \hbar + 2\pi in$, $n = 0, 1, \dots, L-1$, of $\chi_{+\hbar}^{\text{total}}(\mathbf{u}_k|_+)$ or $\chi_{-\hbar}^{\text{total}}(\mathbf{u}_k|_-)$, we obtain

$$(4.4) \quad \chi_{\pm\hbar}^{\text{total}}(\mathbf{u}_k|_{\pm}) - \sum_{a=1}^k \left(\sum_{i=1}^{I_a-1} e^{\pm u_a|_{\pm} \mp m_i - \frac{\gamma}{2}} + \sum_{i=I_a+1}^L e^{\mp u_a|_{\pm} \pm m_i - \frac{\gamma}{2}} - \sum_{a < b}^k \left(e^{\mp u_{a,b}|_{\pm}} + e^{\pm u_{a,b}|_{\pm} + \gamma} \right) \right),$$

which follows from the following lemma.

Lemma 4.1 ([3]). *For any parameters x and \hbar , and integers I and L , performing the shift of parameters*

$$(4.5) \quad x \rightarrow x + I \frac{\hbar}{L}, \quad \hbar \rightarrow \frac{\hbar}{L}, \quad -L+1 \leq I \leq L-1,$$

in $e^{\pm x}/(1 - e^{\pm\hbar})$, leads to the \mathbb{Z}_L invariant part

$$(4.6) \quad \frac{e^{\pm x}}{1 - e^{\pm\hbar}} \longrightarrow \begin{cases} \frac{e^{\pm x}}{1 - e^{\pm\hbar}} & \text{if } -L+1 \leq I \leq 0, \\ \frac{e^{\pm x}}{1 - e^{\pm\hbar}} - e^{\pm x} & \text{if } 1 \leq I \leq L-1 \end{cases}$$

Proof. By

$$\frac{1}{1 - e^{\frac{\hbar}{L}}} = \frac{1 + e^{\frac{\hbar}{L}} + e^{2\frac{\hbar}{L}} + \dots + e^{(L-1)\frac{\hbar}{L}}}{1 - e^{\hbar}},$$

the lemma is proved. \square

Symmetrizing in the variables \mathbf{u}_k , the contribution of a defect inserted at the north (resp. south) pole of S_{\hbar}^2 to the integrand of the JK contour integral ⁵ is $\psi_{\mathbf{I}_k}^{(L)}(\mathbf{u}_k|_+; \mathbf{m}_L)$ (resp. $\psi_{\mathbf{I}_k}^{(L)}(\mathbf{u}_k|_-; \mathbf{m}_L^{\vee})$ with $I_a^{\vee} = L - I_a + 1$ and $m_i^{\vee} = m_{L-i+1}$), where

$$(4.7) \quad \psi_{\mathbf{I}_k}^{(L)}(\mathbf{u}_k; \mathbf{m}_L) = \text{Sym}_{\mathbf{u}_k} \frac{\prod_{a=1}^k \left(\prod_{i=1}^{I_a-1} \left(u_a - m_i - \frac{\gamma}{2} \right) \cdot \prod_{i=I_a+1}^L \left(-u_a + m_i - \frac{\gamma}{2} \right) \right)}{\prod_{a < b}^k u_{b,a} \left(u_{a,b} + \gamma \right)}$$

⁵ In the sequel, we will also simply say ‘the (orbifold) defect’, rather than ‘the contribution of the (orbifold) defect to the integrand of the JK contour integral representation of the gauge theory partition function’.

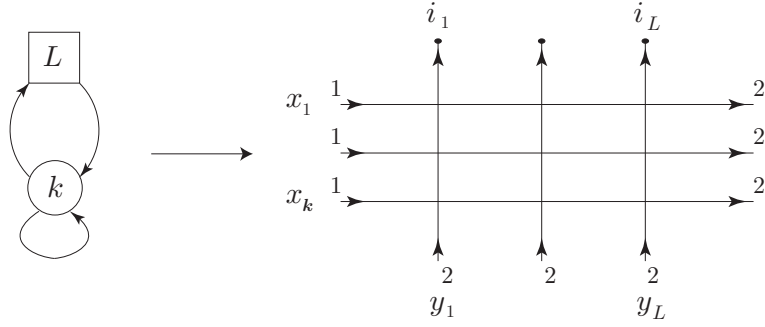


FIGURE 3. The $\mathfrak{su}(2)$ lattice configuration which describes the orbifold defect (4.8) for the A_1 quiver. Here $k \leq L$, and the indices $i_\ell \in \{1, 2\}$, $\ell = 1, \dots, L$, represent spin-states, or equivalently, *colours*.

Here $\text{Sym}_{\mathbf{u}_k}$ stands for the symmetrization of a function $f(\mathbf{u}_k)$ in the variables \mathbf{u}_k ,

$$\text{Sym}_{\mathbf{u}_k} f(\mathbf{u}_k) = \sum_{\sigma \in \mathfrak{S}_k} f(u_{\sigma(1)}, \dots, u_{\sigma(k)}),$$

and \mathfrak{S}_k is the symmetric group of degree k .

Proposition 4.2 ([1, 2, 3]). *Consider a normalization of the A_1 quiver orbifold defect as*

$$(4.8) \quad \begin{aligned} \widehat{\psi}_{\mathbf{I}_k}^{(L)}(\mathbf{u}_k; \mathbf{m}_L) &= (-1)^{kL + \sum_{a=1}^k I_a} \prod_{a < b}^k \left(\gamma^2 - u_{a,b}^2 \right) \times \psi_{\mathbf{I}_k}^{(L)}(\mathbf{u}_k; \mathbf{m}_L) \\ &= \text{Sym}_{\mathbf{u}_k} \omega_{\mathbf{I}_k}^{(L)}(\mathbf{u}_k; \mathbf{m}_L), \end{aligned}$$

where

$$(4.9) \quad \omega_{\mathbf{I}_k}^{(L)}(\mathbf{u}_k; \mathbf{m}_L) = \prod_{a=1}^k \left(\prod_{i=1}^{I_a-1} \left(u_a - m_i - \frac{\gamma}{2} \right) \times \prod_{i=I_a+1}^L \left(u_a - m_i + \frac{\gamma}{2} \right) \right) \times \prod_{a < b}^k \frac{u_{a,b} - \gamma}{u_{a,b}}$$

Then, the defect $\widehat{\psi}_{\mathbf{I}_k}^{(L)}(\mathbf{u}_k; \mathbf{m}_L)$ gives the coordinate Bethe wavefunction of $\mathfrak{su}(2)$ XXX spin- $\frac{1}{2}$ chain.

Note that the defects inserted at the north pole and the south pole of S_h^2 are given by

$$\widehat{\psi}_{\mathbf{I}_k}^{(L)} \left(\mathbf{u}_k |_{+}; \mathbf{m}_L \right) \quad \text{and} \quad \widehat{\psi}_{\mathbf{I}_k^\vee}^{(L)} \left(\mathbf{u}_k |_{-}; \mathbf{m}_L^\vee \right),$$

respectively, where $I_a^\vee = L - I_a + 1$ and $m_i^\vee = m_{L-i+1}$.

Remark 4.3. Proposition 4.2 implies that, setting $u_a = x_a + 1/2$, $m_i = y_i$, and $\gamma = 1$, the defect $\widehat{\psi}_{\mathbf{I}_k}^{(L)}(\mathbf{u}_k; \mathbf{m}_L)$ in (4.8) agrees with the partition function (B.7) for the lattice configuration in Figure 3 of the rational $\mathfrak{su}(2)$ six-vertex model, where the set \mathbf{I}_L labels the positions ℓ of colours $i_\ell \in \{1, 2\}$, and the set \mathbf{I}_k labels the positions k of colour 1.

Remark 4.4. We have derived $\widehat{\psi}_{\mathbf{I}_k}^{(L)}(\mathbf{u}_k; \mathbf{m}_L)$ from the character in (4.4), using (2.7). Using (2.8) instead of (2.7), we obtain the coordinate Bethe wavefunction of the $\mathfrak{su}(2)$ XXZ spin- $\frac{1}{2}$ chain, and (4.9) is replaced by

$$(4.10) \quad \omega_{\mathbf{I}_k}^{K,(L)}(\mathbf{u}_k; \mathbf{m}_L) = \prod_{a=1}^k \left(\prod_{i=1}^{I_a-1} \left[u_a - m_i - \frac{\gamma}{2} \right] \times \prod_{i=I_a+1}^L \left[u_a - m_i + \frac{\gamma}{2} \right] \right) \times \prod_{a < b}^k \frac{[u_{a,b} - \gamma]}{[u_{a,b}]},$$

where $[x] = 2 \sinh(x/2)$.

From the orbifold defect $\widehat{\psi}_{\mathbf{I}_k}^{(L)}(\mathbf{u}_k; \mathbf{m}_L)$, one obtains the $\mathfrak{su}(2)$ six-vertex model partial domain wall partition function (DWPF) [17]. In Appendix A, we prove the following proposition as a corollary of Propositions 4.2 and A.4.

Proposition 4.5 (A_1 partial DWPF). *Summing over the ordered set \mathbf{I}_k in the orbifold defect $\widehat{\psi}_{\mathbf{I}_k}^{(L)}(\mathbf{u}_k; \mathbf{m}_L)$, we define a partition function*

$$(4.11) \quad \widehat{\mathcal{Z}}_k(\mathbf{u}_k; \mathbf{m}_L) = \sum_{\mathbf{I}_k \subset \{1, \dots, L\}} \widehat{\psi}_{\mathbf{I}_k}^{(L)}(\mathbf{u}_k; \mathbf{m}_L)$$

Then, the partition function $\widehat{\mathcal{Z}}_k(\mathbf{u}_k; \mathbf{m}_L)$ agrees with the $\mathfrak{su}(2)$ six-vertex model partial DWPF, which has the determinant expression [17],

$$(4.12) \quad \widehat{\mathcal{Z}}_k(\mathbf{u}_k; \mathbf{m}_L) = \frac{\prod_{a=1}^k \prod_{i=1}^L \left(u_a - m_i - \frac{\gamma}{2} \right) \left(u_a - m_i + \frac{\gamma}{2} \right)}{\prod_{a < b}^k (u_b - u_a) \cdot \prod_{i < j}^L (m_i - m_j)} \times \begin{vmatrix} \frac{1}{\left(u_1 - m_1 - \frac{\gamma}{2} \right) \left(u_1 - m_1 + \frac{\gamma}{2} \right)} & \cdots & \frac{1}{\left(u_1 - m_L - \frac{\gamma}{2} \right) \left(u_1 - m_L + \frac{\gamma}{2} \right)} \\ \vdots & & \vdots \\ \frac{1}{\left(u_k - m_1 - \frac{\gamma}{2} \right) \left(u_k - m_1 + \frac{\gamma}{2} \right)} & \cdots & \frac{1}{\left(u_k - m_L - \frac{\gamma}{2} \right) \left(u_k - m_L + \frac{\gamma}{2} \right)} \\ m_1^{L-k-1} & \cdots & m_L^{L-k-1} \\ \vdots & & \vdots \\ m_1^0 & \cdots & m_L^0 \end{vmatrix},$$

or equally [18, 19],

$$(4.13) \quad \widehat{\mathcal{Z}}_k(\mathbf{u}_k; \mathbf{m}_L) = \frac{\prod_{a=1}^k \prod_{i=1}^L \left(u_a - m_i + \frac{\gamma}{2} \right)}{\prod_{a < b}^k (u_b - u_a)} \times \det \left(u_a^{b-1} \prod_{i=1}^L \frac{u_a - m_i - \frac{\gamma}{2}}{u_a - m_i + \frac{\gamma}{2}} - (u_a - \gamma)^{b-1} \right)_{a,b=1, \dots, k}$$

4.2. Orbifold defect for a simple A_M quiver. We extend the above construction of the A_1 quiver orbifold defects to the simple A_M linear quiver in Figure 2, with the matter content in Table 1. The equivariant characters are given in (3.1), with $L_p = 0$, $p = 1, \dots, M-1$, and $k_1 \leq k_2 \leq \dots \leq k_M \leq L$. To construct orbifold defects which break the gauge symmetry

$U(k_1) \times \cdots \times U(k_M)$ and the flavor symmetry $U(L)$ to a maximal torus, as a generalization of the change of parameters (4.2), we consider

$$(4.14) \quad m_i \rightarrow m_i + \left(i - 1\right) \frac{\hbar}{L}, \quad u_a^{(p)}|_{\pm} \rightarrow u_a^{(p)}|_{\pm} + \left(I_a^{(p)} - 1\right) \frac{\hbar}{L}, \quad \hbar \rightarrow \frac{\hbar}{L},$$

in the total equivariant character $\chi_{+\hbar}^{\text{total}}(\mathbf{u}_{\mathbf{k}}^M|_+)$ or $\chi_{-\hbar}^{\text{total}}(\mathbf{u}_{\mathbf{k}}^M|_-)$ in (2.5), where

$$(4.15) \quad \mathbf{I}_{k_1}^{(1)} \subset \mathbf{I}_{k_2}^{(2)} \subset \cdots \subset \mathbf{I}_{k_M}^{(M)} \subset \mathbf{I}_L = \{1, \dots, L\}, \quad \mathbf{I}_{k_p}^{(p)} = \{I_1^{(p)}, \dots, I_{k_p}^{(p)}\}, \quad I_a^{(p)} < I_{a+1}^{(p)},$$

Taking the \mathbb{Z}_L invariant part of the total equivariant character under $\hbar \rightarrow \hbar + 2\pi i n$, $n = 0, 1, \dots, L - 1$, from Lemma 4.1 one finds

$$(4.16) \quad \begin{aligned} & \chi_{\pm\hbar}^{\text{total}} \left(\mathbf{u}_{\mathbf{k}}^M |_{\pm} \right) \\ & - \sum_{a=1}^{k_M} \left[\sum_{i=1}^{I_a^{(M)}-1} e^{\pm u_a^{(M)}|_{\pm} \mp m_i - \frac{\gamma}{2}} + \sum_{i=I_a^{(M)}+1}^L e^{\mp u_a^{(M)}|_{\pm} \pm m_i - \frac{\gamma}{2}} \right] \\ & + \sum_{p=1}^M \sum_{a < b}^{k_p} \left(e^{\mp u_{a,b}^{(p)}|_{\pm}} + e^{\pm u_{a,b}^{(p)}|_{\pm} + \gamma} \right) \\ & - \sum_{p=1}^{M-1} \sum_{a=1}^{k_p} \left[\sum_{b=1}^{\tilde{I}_a^{(p)}-1} e^{\pm u_a^{(p)}|_{\pm} \mp u_b^{(p+1)}|_{\pm} - \frac{\gamma}{2}} + \sum_{b=\tilde{I}_a^{(p)}+1}^{k_{p+1}} e^{\mp u_a^{(p)}|_{\pm} \pm u_b^{(p+1)}|_{\pm} - \frac{\gamma}{2}} \right], \end{aligned}$$

where the set $\tilde{\mathbf{I}}_a^{(p)}$ is defined by the map

$$(4.17) \quad \mathbf{I}_{k_p}^{(p)} \subset \mathbf{I}_{k_{p+1}}^{(p+1)} \rightarrow \tilde{\mathbf{I}}_{k_p}^{(p)} = \{\tilde{I}_1^{(p)}, \dots, \tilde{I}_{k_p}^{(p)}\} \subset \{1, \dots, k_{p+1}\},$$

which can be explained as follows. $\mathbf{I}_{k_p}^{(p)}$ is a subset in the set $\mathbf{I}_{k_{p+1}}^{(p+1)}$, and $\tilde{\mathbf{I}}_{k_p}^{(p)}$ is a subset in the set $\{1, \dots, k_{p+1}\}$. Mapping the set $\mathbf{I}_{k_{p+1}}^{(p+1)}$ to the set $\{1, \dots, k_{p+1}\}$ using the map $I_a^{(p+1)} \mapsto a$, $a = 1, \dots, p+1$, induces a map from the subset $\mathbf{I}_{k_p}^{(p)}$ to the subset $\tilde{\mathbf{I}}_{k_p}^{(p)}$, which defines $\tilde{\mathbf{I}}_{k_p}^{(p)}$. By (2.7), after symmetrization in the vector multiplet scalars $\mathbf{u}_{k_1}, \dots, \mathbf{u}_{k_M}$, one obtains the defect

$$(4.18) \quad \begin{aligned} & \psi_{\mathbf{I}_{\mathbf{k}}^M}^{(L)} \left(\mathbf{u}_{\mathbf{k}}^M; \mathbf{m}_L \right) \\ & = \text{Sym}_{\mathbf{u}_{k_1}^{(1)}, \dots, \mathbf{u}_{k_M}^{(M)}} \prod_{p=1}^{M-1} \frac{\prod_{a=1}^{k_p} \left(\prod_{b=1}^{\tilde{I}_a^{(p)}-1} \left(u_a^{(p)} - u_b^{(p+1)} - \frac{\gamma}{2} \right) \cdot \prod_{b=\tilde{I}_a^{(p)}+1}^{k_{p+1}} \left(-u_a^{(p)} + u_b^{(p+1)} - \frac{\gamma}{2} \right) \right)}{\prod_{a < b}^{k_p} u_{b,a}^{(p)} \left(u_{a,b}^{(p)} + \gamma \right)} \\ & \quad \times \frac{\prod_{a=1}^{k_M} \left(\prod_{i=1}^{I_a^{(M)}-1} \left(u_a^{(M)} - m_i - \frac{\gamma}{2} \right) \cdot \prod_{i=I_a^{(M)}+1}^L \left(-u_a^{(M)} + m_i - \frac{\gamma}{2} \right) \right)}{\prod_{a < b}^{k_M} u_{b,a}^{(M)} \left(u_{a,b}^{(M)} + \gamma \right)}, \end{aligned}$$

which generalizes $\psi_{\mathbf{I}_{\mathbf{k}}}^{(L)}(\mathbf{u}_{\mathbf{k}}; \mathbf{m}_L)$ in (4.7), where $\mathbf{I}_{\mathbf{k}}^M = \{\mathbf{I}_{k_1}^{(1)}, \dots, \mathbf{I}_{k_M}^{(M)}\}$, and

$$\text{Sym}_{\mathbf{u}_{k_1}^{(1)}, \dots, \mathbf{u}_{k_M}^{(M)}} = \text{Sym}_{\mathbf{u}_{k_1}^{(1)}} \cdots \text{Sym}_{\mathbf{u}_{k_M}^{(M)}}$$

Using a normalization similar to that in (4.8), we find the following proposition.

Proposition 4.6. *The orbifold defect, for the simple A_M quiver in Figure 2,*

$$(4.19) \quad \widehat{\psi}_{\mathbf{I}_k^M}^{(L)} \left(\mathbf{u}_k^M; \mathbf{m}_L \right) = \text{Sym}_{\mathbf{u}_{k_1}^{(1)}, \dots, \mathbf{u}_{k_M}^{(M)}} \prod_{p=1}^{M-1} \omega_{\widehat{\mathbf{I}}_{k_p}^{(p)}}^{(k_{p+1})} \left(\mathbf{u}_{k_p}^{(p)}; \mathbf{u}_{k_{p+1}}^{(p+1)} \right) \times \omega_{\mathbf{I}_{k_M}^{(M)}}^{(L)} \left(\mathbf{u}_{k_M}^{(M)}; \mathbf{m}_L \right),$$

gives the nested coordinate Bethe wavefunction (see e.g. [20]) in the $\mathfrak{su}(M+1)$ XXX spin-chain with spins in the fundamental representation, where $\omega_{\mathbf{I}_k}^{(L)}(\mathbf{u}_k; \mathbf{m}_L)$ is defined in (4.9).

Remark 4.7. Proposition 4.6 implies that, by the change of variables (B.2), the orbifold defect (4.19) coincides with the partition function (B.7) of a lattice configuration, with $L_i = 0$, $i = 1, \dots, M-1$, and $L_M = L$, of the rational $\mathfrak{su}(M+1)$ XXX vertex model, where the set \mathbf{I}_L labels the positions ℓ of all colours $i_\ell \in \{1, \dots, M+1\}$, the set $\mathbf{I}_{k_1}^{(1)}$ labels the positions of colour 1, and the set $\mathbf{I}_{k_p}^{(p)} \setminus \mathbf{I}_{k_{p-1}}^{(p-1)}$, $p = 2, \dots, M$, labels the positions of colour p .

Remark 4.8. In [21], the orbifold defect (4.19) was geometrically constructed as an element in a stable basis [22] in the cotangent bundle of a partial flag variety (see also [23, 24]).

Remark 4.9. Similarly to Remark 4.4, replacing $\omega_{\mathbf{I}_k}^{(L)}(\mathbf{u}_k; \mathbf{m}_L)$ with $\omega_{\mathbf{I}_k}^{K,(L)}(\mathbf{u}_k; \mathbf{m}_L)$ in the orbifold defect (4.19), one obtains the trigonometric expression which coincides with coordinate Bethe wavefunction of the corresponding XXZ spin-chain.

Proposition 4.10. *Summing over the ordered sets \mathbf{I}_k^M , with a fixed set $\mathbf{I}_{k_M}^{(M)}$, in the defect (4.19), we define a partition function*

$$(4.20) \quad \widehat{\mathcal{Z}}_{\mathbf{I}_{k_M}^{(M)}} \left(\mathbf{u}_k^M; \mathbf{m}_L \right) = \sum_{\mathbf{I}_{k_1}^{(1)} \subset \mathbf{I}_{k_2}^{(2)} \subset \dots \subset \mathbf{I}_{k_M}^{(M)}} \widehat{\psi}_{\mathbf{I}_k^M}^{(L)} \left(\mathbf{u}_k^M; \mathbf{m}_L \right)$$

Then, the partition function factorizes into the A_1 quiver orbifold defect in (4.8) and the $\mathfrak{su}(2)$ six-vertex model partial DWPF (4.11),

$$(4.21) \quad \widehat{\mathcal{Z}}_{\mathbf{I}_{k_M}^{(M)}} \left(\mathbf{u}_k^M; \mathbf{m}_L \right) = \prod_{p=1}^{M-1} \widehat{\mathcal{Z}}_{k_p} \left(\mathbf{u}_{k_p}^{(p)}; \mathbf{u}_{k_{p+1}}^{(p+1)} \right) \times \widehat{\psi}_{\mathbf{I}_{k_M}^{(M)}}^{(L)} \left(\mathbf{u}_{k_M}^{(M)}; \mathbf{m}_L \right)$$

Further,

$$(4.22) \quad \sum_{\mathbf{I}_{k_M}^{(M)} \subset \{1, \dots, L\}} \widehat{\mathcal{Z}}_{\mathbf{I}_{k_M}^{(M)}} \left(\mathbf{u}_k^M; \mathbf{m}_L \right) = \prod_{p=1}^{M-1} \widehat{\mathcal{Z}}_{k_p} \left(\mathbf{u}_{k_p}^{(p)}; \mathbf{u}_{k_{p+1}}^{(p+1)} \right) \times \widehat{\mathcal{Z}}_{k_M} \left(\mathbf{u}_{k_M}^{(M)}; \mathbf{m}_L \right)$$

Proof. From **3** in Proposition A.3 and (A.2), the partition function $\widehat{\mathcal{Z}}_{k_1}(\mathbf{u}_{k_1}^{(1)}; \mathbf{u}_{k_2}^{(2)})$ is a symmetric polynomial of $\mathbf{u}_{k_2}^{(2)}$, and then,

$$(4.23) \quad \text{Sym}_{\mathbf{u}_{k_2}^{(2)}} \widehat{\mathcal{Z}}_{k_1} \left(\mathbf{u}_{k_1}^{(1)}; \mathbf{u}_{k_2}^{(2)} \right) \omega_{\widehat{\mathbf{I}}_{k_2}^{(2)}}^{(k_3)} \left(\mathbf{u}_{k_2}^{(2)}; \mathbf{u}_{k_3}^{(3)} \right) = \widehat{\mathcal{Z}}_{k_1} \left(\mathbf{u}_{k_1}^{(1)}; \mathbf{u}_{k_2}^{(2)} \right) \widehat{\psi}_{\widehat{\mathbf{I}}_{k_2}^{(2)}}^{(k_3)} \left(\mathbf{u}_{k_2}^{(2)}; \mathbf{u}_{k_3}^{(3)} \right)$$

Repeating this symmetrization, one finds the factorizations (4.21) and (4.22). \square

| IIA | 0 | 1 | 2 | 3 | 4 | 5 | 6 | 7 | 8 | 9 |
|-----|---|---|---|---|---|---|---|---|---|---|
| NS5 | — | — | — | — | — | | | | | |
| D2 | — | — | | | | | — | | | |
| D4 | — | — | | | | | | — | — | — |

| IIB | 0 | 1 | 2 | 3 | 4 | 5 | 6 | 7 | 8 | 9 |
|-----|---|---|---|---|---|---|---|---|---|---|
| NS5 | — | — | — | — | — | — | | | | |
| D3 | — | — | — | | | | — | | | |
| D5 | — | — | — | | | | | — | — | — |

TABLE 4. On the left is a type-IIA brane configuration, and on the right is the type-IIB brane configuration in [16] that corresponds to it by T-duality along the x^2 -direction (see also Figure 4).

Remark 4.11. In [25], the factorization (4.22) was shown for the $\mathfrak{su}(M+1)$ vertex model (see Remark 4.7), and was traced to a property (called ‘*colour-independence*’) of partition functions that satisfy certain boundary conditions.

5. GENERALIZATIONS BY HIGGSING

In Section 5.1, we recall the Higgsing procedure in the A_M quiver in Figure 1 without orbifold defects, in terms of the equivariant characters (3.1). In Sections 5.2 and 5.3, by applying the Higgsing to the orbifold construction in Section 4, we generalize the simple A_M quiver orbifold defect (4.19) to more general A_2 then to A_M quiver orbifold defects. In Section 5.4, we study the dual of Higgsing on the Bethe side of the Bethe/Gauge correspondence.

5.1. Higgsing. In [16], Gaiotto and Koroteev discussed a Higgsing procedure in terms of type-IIB brane realizations, in 3D $\mathcal{N} = 2$ quiver gauge theories that are Bethe/Gauge dual to XXZ spin-chains. In Table 4 and Figure 4, we describe a type-IIA brane configuration, and a type-IIB brane configuration in [16] that corresponds to it by T-duality along the x^2 -direction. By introducing the twisted mass γ in Table 1, which breaks half the supersymmetry, these configurations describe, respectively, 2D $\mathcal{N} = (2, 2)$ quiver gauge theories on the (x^0, x^1) -directions, and 3D $\mathcal{N} = 2$ quiver gauge theories on the (x^0, x^1, x^2) -directions. For the purposes of this work, the basic idea, as described in Figure 4, is

1. to fine-tune the quiver data so that two D4/D5 branes are aligned at the same position in $(x^2, x^3, x^4, x^5)/(x^3, x^4, x^5)$ -directions, and a segment of a D2/D3 brane stretches between them,
2. the D2/D3 segment that stretches between the two aligned D4/D5 branes is taken to infinity in the (x^7, x^8, x^9) -directions, and finally,
3. a sequence of Hanany-Witten moves of the two aligned D4/D5 branes, which are across NS5 branes, are used to simplify the resulting quiver ⁶.

⁶ The Hanany-Witten moves require that there is at most one Dp brane between an NS5 brane and a D(p+2) brane. In the present work, $p = 2$ or 3, and, as in Figure 4, there is indeed at most one D2/D3 brane between an NS5 brane and a D4/D5 brane. The moves also describe the creation/annihilation of branes. In the present

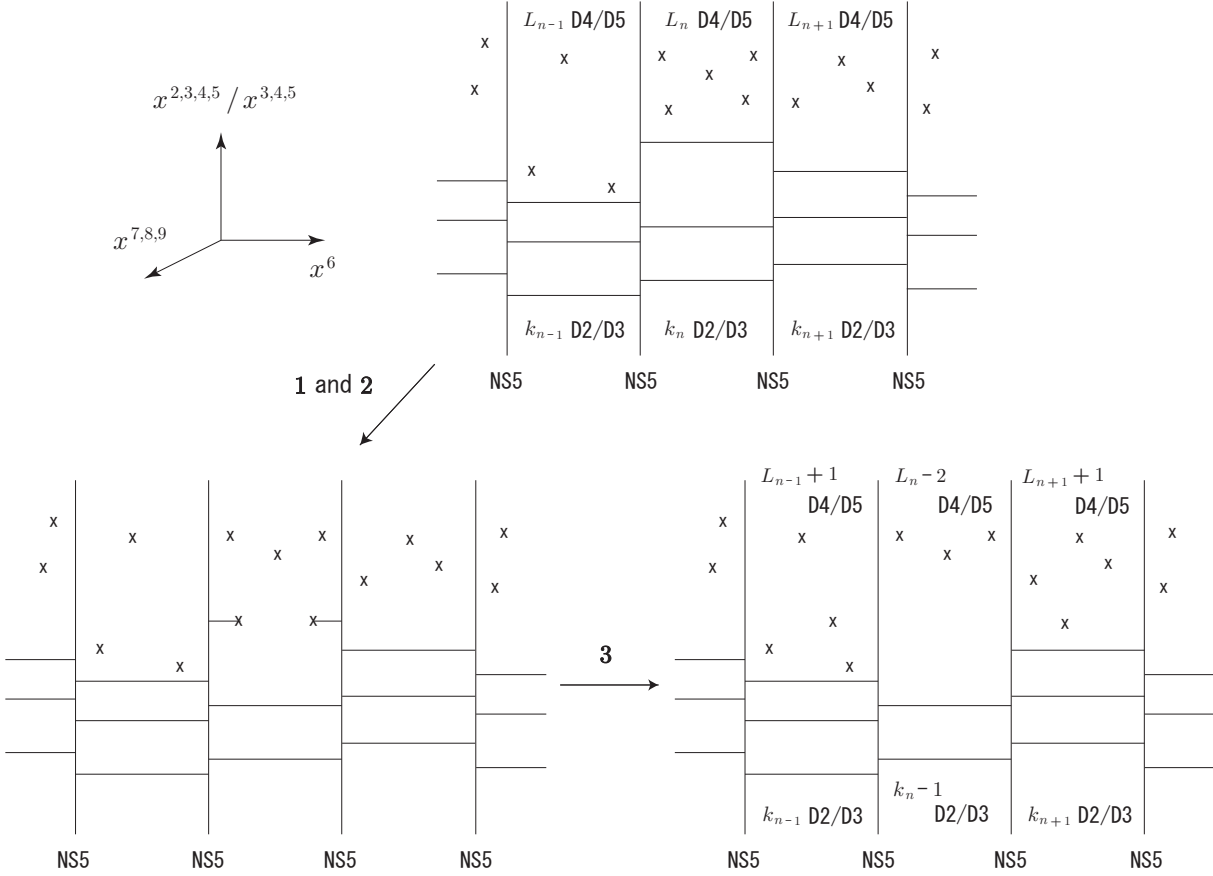


FIGURE 4. The Higgsing procedure including Hanany-Witten moves for type-IIA/IIB brane configuration [16], where the vertical (resp. horizontal) lines represent NS5 (resp. D2/D3) branes, and each x represents a D4/D5 brane. The corresponding quiver description is in Figure 5.

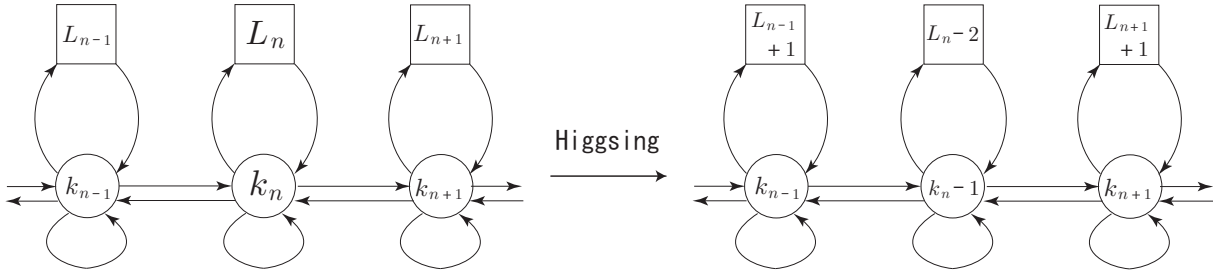


FIGURE 5. Higgsing the n -th gauge node of the A_M linear quiver.

5.1.1. *Higgsing the A_M quiver on the left hand side of Figure 5.* Following [16], the specialization of the parameters

$$(5.1) \quad u_{k_n}^{(n)} = m_{L_{n-1}}^{(n)} - \frac{\gamma}{2} = m_{L_n}^{(n)} + \frac{\gamma}{2} =: \mu_H,$$

work, as in [16], the Higgsing procedure, involves the annihilation of D2/D3 branes, as in Step **3** of Figure 4. We thank A Hanany for discussions on this point.

Higgses the n -th gauge node of the A_M quiver on the left hand side of Figure 5, and changes the quiver parameters as follows,

$$(5.2) \quad \begin{aligned} k_p &\rightarrow k_p, \quad (\text{for } p \neq n), & L_p &\rightarrow L_p, \quad (\text{for } p \neq n, n \pm 1), \\ k_n &\rightarrow k_n - 1, & L_n &\rightarrow L_n - 2, & L_{n \pm 1} &\rightarrow L_{n \pm 1} + 1, \end{aligned}$$

as depicted in the transition from the left hand side to the right hand side of Figure 5 [26].

5.1.2. *Higgsing the equivariant characters* (3.1). Applying (5.1) to the characters, we obtain the Higgsed characters

$$(5.3) \quad \chi_{H,\hbar}^P(\mathbf{u}) := \chi_{\hbar}^P(\mathbf{u})|_{(5.1)},$$

where the following characters remain unchanged

$$(5.4) \quad \begin{aligned} \chi_{H,\hbar}^{V^{(p)}}(\mathbf{u}_{k_p}^{(p)}) &= \chi_{\hbar}^{V^{(p)}}(\mathbf{u}_{k_p}^{(p)}), & \chi_{H,\hbar}^{\Phi^{(p)}}(\mathbf{u}_{k_p}^{(p)}) &= \chi_{\hbar}^{\Phi^{(p)}}(\mathbf{u}_{k_p}^{(p)}), \\ \chi_{H,\hbar}^{X_i^{(p)}}(\mathbf{u}_{k_p}^{(p)}) &= \chi_{\hbar}^{X_i^{(p)}}(\mathbf{u}_{k_p}^{(p)}), & \chi_{H,\hbar}^{Y_i^{(p)}}(\mathbf{u}_{k_p}^{(p)}) &= \chi_{\hbar}^{Y_i^{(p)}}(\mathbf{u}_{k_p}^{(p)}), & \text{for } p \neq n, \\ \chi_{H,\hbar}^{A^{(p')}}(\mathbf{u}_{k_{p'}}^{(p')}, \mathbf{u}_{k_{p'+1}}^{(p'+1)}) &= \chi_{\hbar}^{A^{(p')}}(\mathbf{u}_{k_{p'}}^{(p')}, \mathbf{u}_{k_{p'+1}}^{(p'+1)}), \\ \chi_{H,\hbar}^{B^{(p')}}(\mathbf{u}_{k_{p'}}^{(p')}, \mathbf{u}_{k_{p'+1}}^{(p'+1)}) &= \chi_{\hbar}^{B^{(p')}}(\mathbf{u}_{k_{p'}}^{(p')}, \mathbf{u}_{k_{p'+1}}^{(p'+1)}), & \text{for } p' \neq n-1, n, \end{aligned}$$

while the following characters change

$$(5.5) \quad \begin{aligned} \chi_{H,\hbar}^{V^{(n)}}(\mathbf{u}_{k_n}^{(n)}) &= \chi_{\hbar}^{V^{(n)}}(\mathbf{u}_{k_{n-1}}^{(n)}) - \sum_{a=1}^{k_n-1} \frac{e^{u_a^{(n)} - \mu_H} + e^{-u_a^{(n)} + \mu_H}}{1 - e^{\hbar}}, \\ \chi_{H,\hbar}^{\Phi^{(n)}}(\mathbf{u}_{k_n}^{(n)}) &= \chi_{\hbar}^{\Phi^{(n)}}(\mathbf{u}_{k_{n-1}}^{(n)}) + \sum_{a=1}^{k_n-1} \frac{e^{u_a^{(n)} - \mu_H + \gamma + \hbar} + e^{-u_a^{(n)} + \mu_H + \gamma + \hbar}}{1 - e^{\hbar}} + \frac{e^{\gamma + \hbar}}{1 - e^{\hbar}}, \\ \sum_{i=1}^{L_n} \chi_{H,\hbar}^{X_i^{(n)}}(\mathbf{u}_{k_n}^{(n)}) &= \sum_{i=1}^{L_n-2} \chi_{\hbar}^{X_i^{(n)}}(\mathbf{u}_{k_{n-1}}^{(n)}) + \sum_{a=1}^{k_n-1} \frac{e^{u_a^{(n)} - \mu_H - \gamma} + e^{u_a^{(n)} - \mu_H}}{1 - e^{\hbar}} + \sum_{i=1}^{L_n} \frac{e^{\mu_H - m_i^{(n)} - \frac{\gamma}{2}}}{1 - e^{\hbar}}, \\ \sum_{i=1}^{L_n} \chi_{H,\hbar}^{Y_i^{(n)}}(\mathbf{u}_{k_n}^{(n)}) &= \sum_{i=1}^{L_n-2} \chi_{\hbar}^{Y_i^{(n)}}(\mathbf{u}_{k_{n-1}}^{(n)}) + \sum_{a=1}^{k_n-1} \frac{e^{-u_a^{(n)} + \mu_H} + e^{-u_a^{(n)} + \mu_H - \gamma}}{1 - e^{\hbar}} + \sum_{i=1}^{L_n} \frac{e^{-\mu_H + m_i^{(n)} - \frac{\gamma}{2}}}{1 - e^{\hbar}}, \end{aligned}$$

and

$$\begin{aligned}
\chi_{H,\hbar}^{A^{(n-1)}} \left(\mathbf{u}_{k_{n-1}}^{(n-1)}, \mathbf{u}_{k_n}^{(n)} \right) &= \chi_{\hbar}^{A^{(n-1)}} \left(\mathbf{u}_{k_{n-1}}^{(n-1)}, \mathbf{u}_{k_{n-1}}^{(n)} \right) + \sum_{a=1}^{k_{n-1}} \frac{e^{u_a^{(n-1)} - \mu_H - \frac{\gamma}{2}}}{1 - e^{\hbar}}, \\
\chi_{H,\hbar}^{A^{(n)}} \left(\mathbf{u}_{k_n}^{(n)}, \mathbf{u}_{k_{n+1}}^{(n+1)} \right) &= \chi_{\hbar}^{A^{(n)}} \left(\mathbf{u}_{k_{n-1}}^{(n)}, \mathbf{u}_{k_{n+1}}^{(n+1)} \right) + \sum_{a=1}^{k_{n+1}} \frac{e^{\mu_H - u_a^{(n+1)} - \frac{\gamma}{2}}}{1 - e^{\hbar}}, \\
\chi_{H,\hbar}^{B^{(n-1)}} \left(\mathbf{u}_{k_{n-1}}^{(n-1)}, \mathbf{u}_{k_n}^{(n)} \right) &= \chi_{\hbar}^{B^{(n-1)}} \left(\mathbf{u}_{k_{n-1}}^{(n-1)}, \mathbf{u}_{k_{n-1}}^{(n)} \right) + \sum_{a=1}^{k_{n-1}} \frac{e^{-u_a^{(n-1)} + \mu_H - \frac{\gamma}{2}}}{1 - e^{\hbar}}, \\
\chi_{H,\hbar}^{B^{(n)}} \left(\mathbf{u}_{k_n}^{(n)}, \mathbf{u}_{k_{n+1}}^{(n+1)} \right) &= \chi_{\hbar}^{B^{(n)}} \left(\mathbf{u}_{k_{n-1}}^{(n)}, \mathbf{u}_{k_{n+1}}^{(n+1)} \right) + \sum_{a=1}^{k_{n+1}} \frac{e^{-\mu_H + u_a^{(n+1)} - \frac{\gamma}{2}}}{1 - e^{\hbar}}
\end{aligned} \tag{5.6}$$

The sum of the Higgsed characters in (5.5) becomes

$$\begin{aligned}
(5.7) \quad & \chi_{H,\hbar}^{V^{(n)}} \left(\mathbf{u}_{k_n}^{(n)} \right) + \chi_{H,\hbar}^{\Phi^{(n)}} \left(\mathbf{u}_{k_n}^{(n)} \right) + \sum_{i=1}^{L_n} \left(\chi_{H,\hbar}^{X_i^{(n)}} \left(\mathbf{u}_{k_n}^{(n)} \right) + \chi_{H,\hbar}^{Y_i^{(n)}} \left(\mathbf{u}_{k_n}^{(n)} \right) \right) \\
&= \chi_{\hbar}^{V^{(n)}} \left(\mathbf{u}_{k_{n-1}}^{(n)} \right) + \chi_{\hbar}^{\Phi^{(n)}} \left(\mathbf{u}_{k_{n-1}}^{(n)} \right) + \sum_{i=1}^{L_n-2} \left(\chi_{\hbar}^{X_i^{(n)}} \left(\mathbf{u}_{k_{n-1}}^{(n)} \right) + \chi_{\hbar}^{Y_i^{(n)}} \left(\mathbf{u}_{k_{n-1}}^{(n)} \right) \right) \\
&+ \sum_{a=1}^{k_{n-1}} \left(\frac{e^{-u_a^{(n)} + \mu_H - \gamma}}{1 - e^{\hbar}} - \frac{e^{u_a^{(n)} - \mu_H + \gamma}}{1 - e^{-\hbar}} \right) + \sum_{a=1}^{k_{n-1}} \left(\frac{e^{u_a^{(n)} - \mu_H - \gamma}}{1 - e^{\hbar}} - \frac{e^{-u_a^{(n)} + \mu_H + \gamma}}{1 - e^{-\hbar}} \right) \\
&+ \frac{e^{\gamma + \hbar}}{1 - e^{\hbar}} + \sum_{i=1}^{L_n} \frac{e^{\mu_H - m_i^{(n)} - \frac{\gamma}{2}}}{1 - e^{\hbar}} + \sum_{i=1}^{L_n} \frac{e^{-\mu_H + m_i^{(n)} - \frac{\gamma}{2}}}{1 - e^{\hbar}}
\end{aligned}$$

By considering the partition function (2.7) or (2.8), one finds that the contributions from the second line on the right hand side yield sign factors, while the third line does not depend on the variables $u_a^{(p)}$ and can be decoupled from the quiver gauge theory. One also finds that the extra factors of the first and third (resp. second and fourth) characters in (5.6),

$$(5.8) \quad \sum_{a=1}^{k_{n-1}} \frac{e^{u_a^{(n-1)} - \mu_H - \frac{\gamma}{2}}}{1 - e^{\hbar}} + \sum_{a=1}^{k_{n-1}} \frac{e^{-u_a^{(n-1)} + \mu_H - \frac{\gamma}{2}}}{1 - e^{\hbar}}, \quad \text{resp.} \quad \sum_{a=1}^{k_{n+1}} \frac{e^{u_a^{(n+1)} - \mu_H - \frac{\gamma}{2}}}{1 - e^{\hbar}} + \sum_{a=1}^{k_{n+1}} \frac{e^{-u_a^{(n+1)} + \mu_H - \frac{\gamma}{2}}}{1 - e^{\hbar}},$$

agree with the contributions from extra (anti-)fundamental matter with mass parameter μ_H at the $(n-1)$ -th (resp. $(n+1)$ -th) gauge node. As a result, the transition (5.2), under the specialization (5.1), is confirmed.

5.2. Orbifold defect for A_2 quiver. In this subsection, we apply the Higgsing to the orbifold construction in Section 4 and generalize the simple A_M quiver orbifold defects for $M = 2$ constructed in Section 4.2. The case of general M will be discussed in Section 5.3.

FIGURE 6. Higgsing the A_2 linear quiver.

5.2.1. *Higgsing the A_2 quiver gauge theory in Figure 6.* We set the A_2 quiver data $k_1 \leq k_2 \leq L-1$, so that the specialization (5.1) becomes

$$(5.9) \quad u_{k_2}^{(2)} = m_{L-1} - \frac{\gamma}{2} = m_L + \frac{\gamma}{2} =: \mu_H$$

As before, the twisted masses m_{L-1} and m_L decouple after Higgsing, and compared with the discussion in Section 4.2, one only needs to consider the second factors on the right hand side in the Higgsed characters (5.6).

5.2.2. *Construction of A_2 quiver orbifold defects.* Instead of the change of parameters (4.14), we consider

$$(5.10) \quad \begin{aligned} \mu_H &\rightarrow \mu_H + (L-2) \frac{\hbar}{L-1}, \\ m_i &\rightarrow m_i + (i-1) \frac{\hbar}{L-1}, \quad i = 1, \dots, L-2, \\ u_a^{(1)}|_{\pm} &\rightarrow u_a^{(1)}|_{\pm} + (I_a^{(1)} - 1) \frac{\hbar}{L-1}, \quad a = 1, \dots, k_1, \\ u_a^{(2)}|_{\pm} &\rightarrow u_a^{(2)}|_{\pm} + (I_a^{(2)} - 1) \frac{\hbar}{L-1}, \quad a = 1, \dots, k_2 - 1, \quad \hbar \rightarrow \frac{\hbar}{L-1}, \end{aligned}$$

which is consistent with Higgsing, where

$$(5.11) \quad \mathbf{I}_{k_1}^{(1)} \subset \mathbf{I}_{k_2-1}^{(2)} \uplus \{L-1\} \subset \{1, \dots, L-1\}, \quad I_a^{(p)} < I_{a+1}^{(p)},$$

and the symbol \uplus denotes the pairwise disjoint union. Then, as a generalization of (4.19) for $M = 2$, we obtain an orbifold defect

$$(5.12) \quad \widehat{\psi}_{\mathbf{I}_{k_1}^{(1)}, \mathbf{I}_{k_2-1}^{(2)}}^{(1|1, L-2)} \left(\mathbf{u}_{k_1}^{(1)}, \mathbf{u}_{k_2-1}^{(2)}; \mu_H, \mathbf{m}_{L-2} \right) = \text{Sym}_{\mathbf{u}_{k_1}^{(1)}, \mathbf{u}_{k_2-1}^{(2)}} \omega_{\mathbf{I}_{k_1}^{(1)}}^{(k_2)} \left(\mathbf{u}_{k_1}^{(1)}; \mathbf{u}_{k_2-1}^{(2)}, \mu_H \right) \omega_{\mathbf{I}_{k_2-1}^{(2)}}^{(L-2)} \left(\mathbf{u}_{k_2-1}^{(2)}; \mathbf{m}_{L-2} \right),$$

where $\omega_{\mathbf{I}_k}^{(L)}(\mathbf{u}_k; \mathbf{m}_L)$ is defined in (4.9), and $\tilde{\mathbf{I}}_{k_1}^{(1)}$ is defined by the map (4.17) for $\mathbf{I}_{k_1}^{(1)} \subset \mathbf{I}_{k_2-1}^{(2)} \uplus \{L-1\}$. Note that, instead of the change of parameters (5.10), by considering

$$(5.13) \quad \begin{aligned} \mu_H &\rightarrow \mu_H, \\ m_i &\rightarrow m_i + i \frac{\hbar}{L-1}, \quad i = 1, \dots, L-2, \\ u_a^{(1)}|_{\pm} &\rightarrow u_a^{(1)}|_{\pm} + \left(I_a^{(1)} - 1 \right) \frac{\hbar}{L-1}, \quad a = 1, \dots, k_1, \\ u_a^{(2)}|_{\pm} &\rightarrow u_a^{(2)}|_{\pm} + \left(I_a^{(2)} - 1 \right) \frac{\hbar}{L-1}, \quad a = 1, \dots, k_2 - 1, \quad \hbar \rightarrow \frac{\hbar}{L-1}, \end{aligned}$$

with

$$(5.14) \quad \mathbf{I}_{k_1}^{(1)} \subset \{1\} \uplus \mathbf{I}_{k_2-1}^{(2)} \subset \{1, \dots, L-1\}, \quad I_a^{(p)} < I_{a+1}^{(p)},$$

we obtain an another orbifold defect

$$(5.15) \quad \widehat{\psi}_{\mathbf{I}_{k_1}^{(1)}, \mathbf{I}_{k_2-1}^{(2)}}^{(2|1, L-2)} \left(\mathbf{u}_{k_1}^{(1)}, \mathbf{u}_{k_2-1}^{(2)}; \mu_H, \mathbf{m}_{L-2} \right) = \text{Sym}_{\mathbf{u}_{k_1}^{(1)}, \mathbf{u}_{k_2-1}^{(2)}} \omega_{\tilde{\mathbf{I}}_{k_1}^{(1)}}^{(k_2)} \left(\mathbf{u}_{k_1}^{(1)}; \mu_H, \mathbf{u}_{k_2-1}^{(2)} \right) \omega_{\tilde{\mathbf{I}}_{k_2-1}^{(2)}}^{(L-2)} \left(\mathbf{u}_{k_2-1}^{(2)}; \mathbf{m}_{L-2} \right),$$

where $\tilde{I}_a^{(2)} = I_a^{(2)} - 1$.

5.2.3. More general A_2 quiver orbifold defects. One can apply the above Higgsing procedure repeatedly. Consider the A_2 quiver in Figure 1 with $M = 2$, set $k_1 \leq L_1 + k_2 \leq L_1 + L_2$, and apply the change of parameters

$$(5.16) \quad \begin{aligned} m_i^{(1)} &\rightarrow m_i^{(1)} + \left(L_2 + i - 1 \right) \frac{\hbar}{L_1 + L_2}, \\ m_i^{(2)} &\rightarrow m_i^{(2)} + \left(i - 1 \right) \frac{\hbar}{L_1 + L_2}, \\ u_a^{(p)}|_{\pm} &\rightarrow u_a^{(p)}|_{\pm} + \left(I_a^{(p)} - 1 \right) \frac{\hbar}{L_1 + L_2}, \quad \hbar \rightarrow \frac{\hbar}{L_1 + L_2}, \end{aligned}$$

to the equivariant characters (3.1), with $M = 2$, where

$$(5.17) \quad \mathbf{I}_{k_1}^{(1)} \subset \mathbf{I}_{k_2}^{(2)} \uplus \{L_2 + 1, \dots, L_1 + L_2\} \subset \{1, \dots, L_1 + L_2\}, \quad I_a^{(p)} < I_{a+1}^{(p)}.$$

As a result, we find an orbifold defect for the A_2 quiver,

$$(5.18) \quad \widehat{\psi}_{\mathbf{I}_{k_1}^{(1)}, \mathbf{I}_{k_2}^{(2)}}^{(1|L_1, L_2)} \left(\mathbf{u}_{k_1}^{(1)}, \mathbf{u}_{k_2}^{(2)}; \mathbf{m}_{L_1}^{(1)}, \mathbf{m}_{L_2}^{(2)} \right) = \text{Sym}_{\mathbf{u}_{k_1}^{(1)}, \mathbf{u}_{k_2}^{(2)}} \omega_{\tilde{\mathbf{I}}_{k_1}^{(1)}}^{(L_1+k_2)} \left(\mathbf{u}_{k_1}^{(1)}; \mathbf{u}_{k_2}^{(2)}, \mathbf{m}_{L_1}^{(1)} \right) \omega_{\tilde{\mathbf{I}}_{k_2}^{(2)}}^{(L_2)} \left(\mathbf{u}_{k_2}^{(2)}; \mathbf{m}_{L_2}^{(2)} \right),$$

which generalizes the defect (5.12). Similarly, instead of (5.16), by considering

$$(5.19) \quad \begin{aligned} m_i^{(1)} &\rightarrow m_i^{(1)} + (i-1) \frac{\hbar}{L_1 + L_2}, \\ m_i^{(2)} &\rightarrow m_i^{(2)} + (L_1 + i - 1) \frac{\hbar}{L_1 + L_2}, \\ u_a^{(p)}|_{\pm} &\rightarrow u_a^{(p)}|_{\pm} + (I_a^{(p)} - 1) \frac{\hbar}{L_1 + L_2}, \quad \hbar \rightarrow \frac{\hbar}{L_1 + L_2}, \end{aligned}$$

with

$$(5.20) \quad \mathbf{I}_{k_1}^{(1)} \subset \{1, \dots, L_1\} \uplus \mathbf{I}_{k_2}^{(2)} \subset \{1, \dots, L_1 + L_2\}, \quad I_a^{(p)} < I_{a+1}^{(p)},$$

we find another orbifold defect for the A_2 quiver,

$$(5.21) \quad \widehat{\psi}_{\mathbf{I}_{k_1}^{(1)}, \mathbf{I}_{k_2}^{(2)}}^{(2|L_1, L_2)} \left(\mathbf{u}_{k_1}^{(1)}, \mathbf{u}_{k_2}^{(2)}; \mathbf{m}_{L_1}^{(1)}, \mathbf{m}_{L_2}^{(2)} \right) = \text{Sym}_{\mathbf{u}_{k_1}^{(1)}, \mathbf{u}_{k_2}^{(2)}} \omega_{\widetilde{\mathbf{I}}_{k_1}^{(1)}}^{(L_1+k_2)} \left(\mathbf{u}_{k_1}^{(1)}; \mathbf{m}_{L_1}^{(1)}, \mathbf{u}_{k_2}^{(2)} \right) \omega_{\widetilde{\mathbf{I}}_{k_2}^{(2)}}^{(L_2)} \left(\mathbf{u}_{k_2}^{(2)}; \mathbf{m}_{L_2}^{(2)} \right),$$

which generalizes the defect (5.15), where $\widetilde{I}_a^{(2)} = I_a^{(2)} - L_1$.

5.3. Orbifold defect for A_M quiver. It is straightforward to generalize the above constructions of the orbifold defects (5.18) and (5.21) to the A_M quiver in Figure 1 (see Table 1 for the matter content), where we set

$$(5.22) \quad k_p \leq L_p + k_{p+1}, \quad k_M \leq L_M, \quad p = 1, \dots, M-1$$

The orbifold defects for the A_2 quiver are composed of the orbifold defect $\omega_{\mathbf{I}_k}^{(L)}(\mathbf{u}_k; \mathbf{m}_L)$ in (4.9) for the A_1 quiver, and it is useful to define

$$(5.23) \quad \begin{aligned} \omega_{\mathbf{I}_k}^{(1|\ell+L)}(\mathbf{u}_k; \mathbf{v}_\ell, \mathbf{m}_L) &:= \omega_{\mathbf{I}_k}^{(\ell+L)}(\mathbf{u}_k; \mathbf{v}_\ell, \mathbf{m}_L), \\ \omega_{\mathbf{I}_k}^{(2|\ell+L)}(\mathbf{u}_k; \mathbf{v}_\ell, \mathbf{m}_L) &:= \omega_{\mathbf{I}_k}^{(\ell+L)}(\mathbf{u}_k; \mathbf{m}_L, \mathbf{v}_\ell) \end{aligned}$$

Now, from the equivariant characters (3.1), we find orbifold defects for the A_M quiver, which generalize the simple A_M quiver orbifold defect (4.19),

$$(5.24) \quad \widehat{\psi}_{\mathbf{I}_k^M}^{(S|L)} \left(\mathbf{u}_k^M; \mathbf{m}_L^M \right) = \text{Sym}_{\mathbf{u}_{k_1}^{(1)}, \dots, \mathbf{u}_{k_M}^{(M)}} \prod_{p=1}^{M-1} \omega_{\widetilde{\mathbf{I}}_{k_p}^{(p)}}^{(s_p|k_{p+1}+L_p)} \left(\mathbf{u}_{k_p}^{(p)}; \mathbf{u}_{k_{p+1}}^{(p+1)}, \mathbf{m}_{L_p}^{(p)} \right) \times \omega_{\widetilde{\mathbf{I}}_{k_M}^{(M)}}^{(L_M)} \left(\mathbf{u}_{k_M}^{(M)}; \mathbf{m}_{L_M}^{(M)} \right),$$

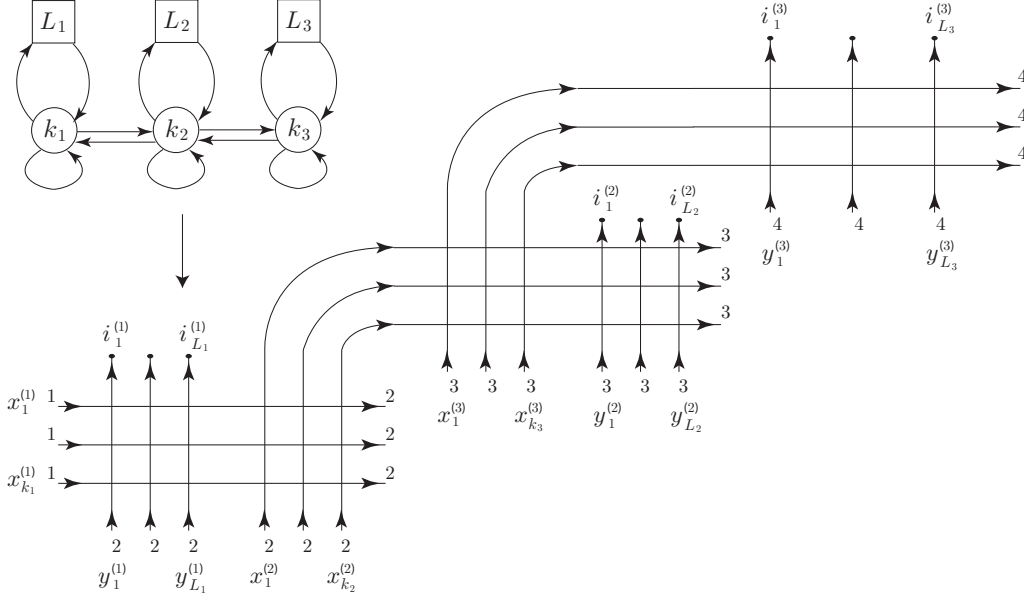


FIGURE 7. An $\mathfrak{su}(4)$ lattice configuration with $s_1 = 2, s_2 = 1$ which describes the orbifold defect (5.29) for the A_3 quiver. Here $k_1 \leq L_1 + k_2, k_2 \leq L_2 + k_3, k_3 \leq L_3$ and $i_\ell^{(p)} \in \{1, \dots, p+1\}, \ell = 1, \dots, L_p, p = 1, 2, 3$ represent colours.

which is characterized by the set $\mathbf{S} = \{s_1, \dots, s_{M-1}\}$, $s_p \in \{1, 2\}$, and the sets \mathbf{I}_k^M , with the inclusion relations

$$(5.25) \quad \begin{aligned} \mathbf{I}_{k_p}^{(p)} \subset \widehat{\mathbf{I}}_{k_{p+1}+L_p}^{(p+1)} &:= \begin{cases} \mathbf{I}_{k_{p+1}}^{(p+1)} \uplus \{L_p^{(\mathbf{S})} + L_{p+1} + 1, \dots, L_p^{(\mathbf{S})} + L_p + L_{p+1}\} & \text{if } s_p = 1, \\ \{L_p^{(\mathbf{S})} + 1, \dots, L_p^{(\mathbf{S})} + L_p\} \uplus \mathbf{I}_{k_{p+1}}^{(p+1)} & \text{if } s_p = 2, \end{cases} \\ &\subset \{L_p^{(\mathbf{S})} + 1, \dots, L_p^{(\mathbf{S})} + L_p + L_{p+1}\}, \quad p = 1, \dots, M-1, \\ \mathbf{I}_{k_M}^{(M)} \subset \widehat{\mathbf{I}}_{L_M}^{(M+1)} &:= \{L_M^{(\mathbf{S})} + 1, \dots, L_M^{(\mathbf{S})} + L_M\} \end{aligned}$$

Here $L_p^{(\mathbf{S})} = \sum_{q=1}^{p-1} L_q \delta_{s_q, 2}$, and the sets $\widetilde{\mathbf{I}}_k^M$ are defined by the map (4.17), for the above inclusion relations. We claim that, by the reparametrizations (B.2), the orbifold defect (5.24) coincides with the partition function (B.7) for a lattice configuration of the $\mathfrak{su}(M+1)$ vertex model,

$$(5.26) \quad \widehat{\psi}_{\mathbf{I}_k^M}^{(\mathbf{S}|\mathbf{L})} \left(\mathbf{u}_k^M; \mathbf{m}_L^M \right) = \widehat{\psi}_{L, i_L^M}^{(\mathbf{S}|\mathbf{L})} \left(\mathbf{x}_k^M; \mathbf{y}_L^M \right),$$

where $\widehat{\mathbf{I}}_{k_{p+1}+L_p}^{(p+1)} \setminus \mathbf{I}_{k_{p+1}}^{(p+1)}$, $p = 1, \dots, M-1$, and $\widehat{\mathbf{I}}_{L_M}^{(M+1)}$ label the positions ℓ of colours $i_\ell^{(p)} \in \{1, \dots, p+1\}$ and $i_\ell^{(M)} \in \{1, \dots, M+1\}$, respectively, the set $\mathbf{I}_{k_1}^{(1)}$ labels the positions of colour 1, the set $\widehat{\mathbf{I}}_{k_p+L_{p-1}}^{(p)} \setminus \mathbf{I}_{k_{p-1}}^{(p-1)}$, $p = 2, \dots, M$, labels the positions of colour p , and the set $\widehat{\mathbf{I}}_{L_M}^{(M+1)} \setminus \mathbf{I}_{k_M}^{(M)}$ labels the positions of colour $M+1$.

Example 5.1. Consider the A_3 quiver in Figure 1, with $M = 3$, and the change of parameters

$$\begin{aligned}
(5.27) \quad m_i^{(1)} &\rightarrow m_i^{(1)} + (i-1) \frac{\hbar}{L_1 + L_2 + L_3}, \\
m_i^{(2)} &\rightarrow m_i^{(2)} + (L_1 + L_3 + i - 1) \frac{\hbar}{L_1 + L_2 + L_3}, \\
m_i^{(3)} &\rightarrow m_i^{(3)} + (L_1 + i - 1) \frac{\hbar}{L_1 + L_2 + L_3}, \\
u_a^{(p)}|_{\pm} &\rightarrow u_a^{(p)}|_{\pm} + \left(I_a^{(p)} - 1 \right) \frac{\hbar}{L_1 + L_2 + L_3}, \quad \hbar \rightarrow \frac{\hbar}{L_1 + L_2 + L_3},
\end{aligned}$$

with

$$\begin{aligned}
(5.28) \quad \mathbf{I}_{k_1}^{(1)} \subset \{1, \dots, L_1\} \uplus \mathbf{I}_{k_2}^{(2)} \subset \{1, \dots, L_1\} \uplus \mathbf{I}_{k_3}^{(3)} \uplus \{L_1 + L_3 + 1, \dots, L_1 + L_2 + L_3\} \\
\subset \{1, \dots, L_1 + L_2 + L_3\},
\end{aligned}$$

where $I_a^{(p)} < I_{a+1}^{(p)}$. Our claim is that the orbifold defect

$$\begin{aligned}
(5.29) \quad \widehat{\psi}_{\mathbf{I}_k^3}^{(2,1|L)} \left(\mathbf{u}_k^3; \mathbf{m}_L^3 \right) \\
= \text{Sym}_{\mathbf{u}_{k_1}^{(1)}, \mathbf{u}_{k_2}^{(2)}, \mathbf{u}_{k_3}^{(3)}} \omega_{\widetilde{\mathbf{I}}_{k_1}^{(1)}}^{(2|k_2+L_1)} \left(\mathbf{u}_{k_1}^{(1)}; \mathbf{u}_{k_2}^{(2)}, \mathbf{m}_{L_1}^{(1)} \right) \omega_{\widetilde{\mathbf{I}}_{k_2}^{(2)}}^{(1|k_3+L_2)} \left(\mathbf{u}_{k_2}^{(2)}; \mathbf{u}_{k_3}^{(3)}, \mathbf{m}_{L_2}^{(2)} \right) \omega_{\widetilde{\mathbf{I}}_{k_3}^{(3)}}^{(L_3)} \left(\mathbf{u}_{k_3}^{(3)}; \mathbf{m}_{L_3}^{(3)} \right),
\end{aligned}$$

coincides with the partition function (B.7) for the $\mathfrak{su}(4)$ lattice configuration in Figure 7 by the reparametrizations (B.2).

Remark 5.2. In the A_M quiver orbifold defects (5.24), by replacing the elementary blocks $\omega_{\mathbf{I}_k}^{(s|\ell+L)}(\mathbf{u}_k; \mathbf{v}_\ell, \mathbf{m}_L)$ in (5.23) with

$$(5.30) \quad \omega_{\mathbf{I}_k}^{(\ell+L)}(\mathbf{u}_k; \mathbf{m}_{L^{(c)}}, \mathbf{v}_\ell, \mathbf{m}_{L-L^{(c)}}),$$

we obtain a further generalization of the orbifold defects, where $\mathbf{m}_{L-L^{(c)}} = \{m_1, \dots, m_{L-L^{(c)}}\}$ and $\mathbf{m}_{L^{(c)}} = \{m_{L-L^{(c)}+1}, \dots, m_L\}$. By this generalization, our claim (5.26) is obviously generalized to a claim for the lattice configurations which mix two lattice configurations in Figure 13 (and Figure 12).

5.4. Higgsing on the Bethe side of the Bethe/Gauge correspondence. As in Appendix B, the lattice configurations of the rational $\mathfrak{su}(M+1)$ vertex model consist of three types of vertices a , b and c in Figure 11 with vertex weights $a(x, y) = x - y + 1$, $b(x, y) = x - y$ and $c(x, y) = 1$. Consider the two types of lattice configurations in Figure 8 consisting of $k+1$ horizontal-line variables x and x_a , $a = 1, \dots, k$, and $L+2$ vertical-line variables w_1, w_2 and y_ℓ , $\ell = 1, \dots, L$.

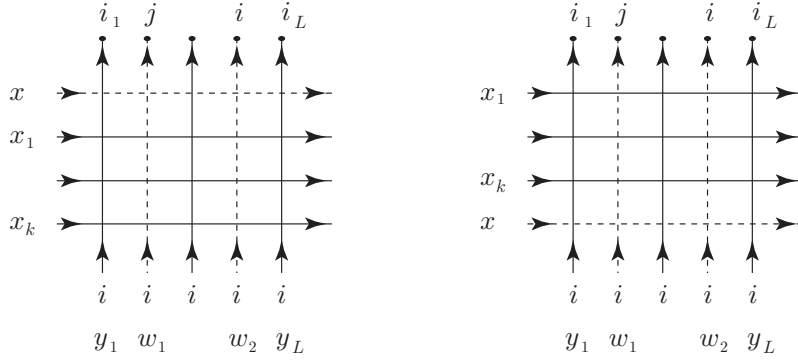


FIGURE 8. Lattice configurations.

The bonds on the lower boundary are assigned the (fixed and same) colour i , and the bonds on the upper boundary are assigned (fixed but varying) colours $i, j, i_\ell, \ell = 1, \dots, L, j < i$. We take the colours s coming from the left boundary to be less than i , i.e. $s < i$, while the colours that remain unspecified (such as those on the bonds on the right boundary) can take any value that is allowed by colour conservation. If the top bond of the left-most vertical line has colour i , then all vertices on this vertical line are of type- b and their weights factor out trivially.

We now consider the Higgsing of the dashed lines by imposing the condition (5.1), where, by the change of variables (B.2) this condition yields

$$(5.31) \quad \text{A-type condition : } x_{k_n}^{(n)} = y_{L_{n-1}}^{(n)} - 1 \quad \text{and} \quad \text{B-type condition : } x_{k_n}^{(n)} = y_{L_n}^{(n)}$$

In other words, $a(x_{k_n}^{(n)}, y_{L_{n-1}}^{(n)}) = 0$ and $b(x_{k_n}^{(n)}, y_{L_n}^{(n)}) = 0$, respectively. For the above two lattice configurations, let us impose the A-type condition $a(x, w_1) = 0$ on the first dashed vertical line and the B-type condition $b(x, w_2) = 0$ on the second dashed vertical line. For the Higgsing, we further consider $x \rightarrow \infty$ limit corresponding to the decoupling of the vector multiplet scalar. With the above conditions, the dominant lattice configuration should be one with the minimal number of c vertices on the dashed lines.

If the intersection of the horizontal dashed line and the vertical dashed line with top boundary colour i is a c vertex, then there are, at least, three (resp. two) c vertices on the dashed lines for the left (resp. right) lattice configuration. To have the minimal number of c vertices, this intersection should be an a vertex by the B-type condition. In fact, in this case, the lattice configurations with minimal number of c vertices are given in Figure 9.

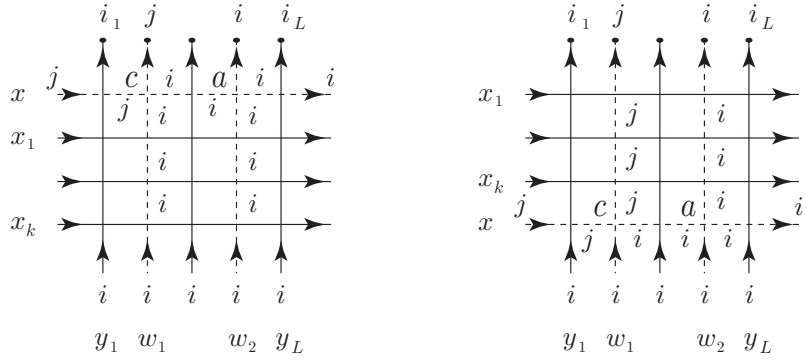


FIGURE 9. Higgsed lattice configurations.

Here, on the dashed lines, there is exactly one c vertex at the intersection of the horizontal dashed line and the vertical dashed line with top boundary colour j . The other vertices on the dashed lines are also uniquely determined, where the left and right side boundary colours of the horizontal dashed line are fixed as j and i , respectively. Note that without the second vertical dashed line with variable w_2 , the lattice configuration on the dashed lines with a minimal number of c vertex is not uniquely determined, and the Higgsing procedure for two vertical lines is inevitable.

Now we consider that the horizontal dashed lines are connected with other lattice configuration in Figure 10.

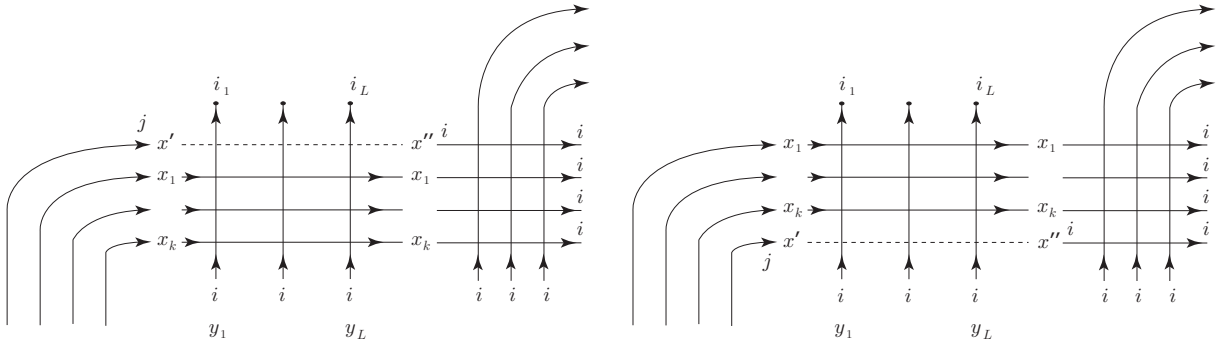


FIGURE 10. Higgsed lattice configurations connected with other lattices.

In this case, before taking the limit $x \rightarrow \infty$, we split this variable into three pieces x , x' and x'' . As we will discuss in Section 6.3, the splitting of the variable x is interpreted as the lattice version of a Hanany-Witten move. Further, we deform the lattice configuration by taking the decoupling limit $x'' \rightarrow \infty$ to remove the horizontal line, with the variable x'' and colour i at the two end boundaries, which uniquely results in no c vertex ⁷.

⁷ On the gauge side, we can interpret taking the limit $x'' \rightarrow \infty$ as the decoupling of a pair of fundamental and anti-fundamental matter, with twisted masses x'' , at the $(n+1)$ -th node after the Hanany-Witten move in Figure 5 (see Section 6.3).

Repeating this process, one can construct the $\mathfrak{su}(M+1)$ lattice configurations in Appendix B (e.g. see Figure 7) from the lattice configuration associated with the simple A_M linear quiver in Figure 2.

6. THE LATTICE VERSIONS OF HIGGSING AND HANANY-WITTEN MOVES

6.1. Korepin's specialization of parameters. A fundamental object in exact computations in spin-chain physics is the domain wall partition function (DWPF) introduced by Korepin, in the $\mathfrak{su}(2)$ spin- $\frac{1}{2}$ six-vertex model [27]. As explained in Appendix A, Korepin proposed a specialization of the parameters (the rapidities and the inhomogeneities) of the DWPF that leads to a recursion relation (and an initial condition) that completely determine it [27]. In [28], Izergin solved Korepin's recursion relation and obtained a determinant expression for the DWPF (see Propositions A.3 and A.4).

6.2. Gaiotto and Koroteev's specialization of parameters as a variation on Korepin's. The specialization (5.1) of the parameters, used in the Higgsing procedure by Gaiotto and Koroteev, is a variation on Korepin's, in the sense that it is essentially the same with two differences between them.

6.2.1. The first difference. Korepin's derivation of the recursion relation requires one type of conditions, and can either, while the Higgsing procedure requires both as in (5.31).

In the case of domain wall boundary conditions, the DWPF is symmetric in the horizontal-line variables and also in the vertical-line variables, and one can choose the variables that one wishes to specialize to be those on lines on the boundaries of the (finite) lattice configuration on which the DWPF is defined. Once we do that, we have more information about the colours of the state variables on these lines, and only one condition is needed to derive the recursion relation.

In the case of Higgsing, when translated to the lattice, one deals with lattice configurations that correspond to the coordinate Bethe wavefunction which is not a symmetric function in the vertical-line (inhomogeneity) variables, one cannot (for general choices of the Higgsing parameters) associate the variables that one wishes to specialize to boundary lattice lines, and one requires (in general) two independent conditions. This makes the specialization of Gaiotto and Koroteev a more general version of Korepin's.

6.2.2. The second difference. In Izergin-Korepin-type computations, one wishes to factor out the (finite) contributions of a single horizontal and a single vertical lattice line (rather than completely trivialize them), so the parameters that are identified by Korepin's conditions are allowed to remain finite.

On the other hand, in the lattice version of Higgsing, one wishes to trivialize the contributions of a single horizontal and two vertical lattice lines, and this is achieved by identifying three parameters

(using two conditions), then taking that parameter to infinity and normalizing appropriately. In the type-IIA/IIB brane realizations in Figure 4, this Higgsing procedure corresponds to Steps **1** and **2**. This makes the specialization of Gaiotto and Koroteev a limiting case of Korepin's.

6.3. The lattice version of the Hanany-Witten moves. One of the ingredients of the Higgsing of Gaiotto and Koroteev is a sequence of Hanany-Witten moves, in the sense that, in the type-IIA/IIB brane realizations in Figure 4, the transition from (anti-)bifundamental matter to new (anti-)fundamental matter is the result of Hanany-Witten moves and described by Step **3** [26, 16]⁸. In Figure 5, the appearance (after Higgsing) of two pairs of fundamental and anti-fundamental matter from the pair of initial (before Higgsing) bifundamental and anti-bifundamental matter is the consequence of a sequence of Hanany-Witten moves. On the lattice side, following the splitting of the variable x in Figure 10 and below, the disappearance of the initial horizontal-line parameter x , and the appearance of two new vertical-line parameters x' and x'' , which is a re-assignment of what were (initially) horizontal-line variables as (new) vertical-line variables, is the lattice version of the Hanany-Witten move.

7. REMARKS

7.1. Affinization. In [29], Bonelli, Sciarappa, Tanzini and Vasko studied connections between 4D $\mathcal{N} = 2$ supersymmetric gauge theories and quantum integrable systems of the hydrodynamic type. In particular, the \widehat{A}_M quiver gauge theory that plays a central role, and appears in Figure 1, in [29], is the affine version of the A_M quiver gauge theory that plays a central role, and appears in Figure 1, in the present work. This leads us to expect that the present work has an affine extension along the lines of [29].

7.2. Quiver with orbifold defects. In Section 4, we considered a \mathbb{Z}_L orbifold of the 2D gauge theory described by the A_M quiver in Figure 2 and obtained the orbifold defect (4.19) labeled by the nested sequences (4.15). In [30], Bonelli, Fasola and Tanzini studied a class of 4D A_1 quiver gauge theories, with a codimension-2 surface defect, that supports *nested instantons* obtained by an orbifold and labeled by nested partitions. They discussed a 2D gauge theory described by a quiver that is different from that used in the present work, and that corresponds to the moduli space of nested instantons. It would be interesting to find the relation, if any, between the two constructions.

ACKNOWLEDGEMENTS

We thank F C Alcaraz, G Bonelli, A Hanany, H Kanno, H C Kim, L Piroli, B Pozsgay, A Tanzini and Y Terashima for discussions and correspondence, and the Australian Research Council for financial support.

⁸ In the case of the A_1 quiver, there is no (anti-)bifundamental matter and no Hanany-Witten moves.

APPENDIX A. THE $\mathfrak{su}(2)$ SIX-VERTEX MODEL PARTIAL DOMAIN WALL PARTITION FUNCTION

We prove Proposition 4.5, to the effect that the partition function $\widehat{\mathcal{Z}}_k(\mathbf{u}_k; \mathbf{m}_L)$ in (4.11), constructed from the orbifold defect $\widehat{\psi}_{\mathbf{I}_k}^{(L)}(\mathbf{u}_k; \mathbf{m}_L)$ in (4.8), agrees with the $\mathfrak{su}(2)$ partial domain wall partition function (DWPF) of the rational six-vertex model.

Lemma A.1. *The orbifold defect $\widehat{\psi}_{\mathbf{I}_k}^{(L)}(\mathbf{u}_k; \mathbf{m}_L)$ and the partition function $\widehat{\mathcal{Z}}_k(\mathbf{u}_k; \mathbf{m}_L)$ are polynomials of degree $L - 1$ in each u_a .*

Proof. We show that $\widehat{\mathcal{Z}}_k(\mathbf{u}_k; \mathbf{m}_L)$ is regular at $u_A = u_B$. Let $\widehat{\sigma}_{A,B}$ be an operator acting on functions of \mathbf{u}_k which exchanges u_A and u_B , and consider the defect $\omega_{\mathbf{I}_k}(\mathbf{u}_k) := \omega_{\mathbf{I}_k}^{(L)}(\mathbf{u}_k; \mathbf{m}_L)$ in (4.9). Symmetrizing in the variables \mathbf{u}_k , the pole at $u_A = u_B$, $A < B$, in $\omega_{\mathbf{I}_k}(\mathbf{u}_k)$ cancels the corresponding pole in $\widehat{\sigma}_{A,B} \cdot \omega_{\mathbf{I}_k}(\mathbf{u}_k)$. Therefore, $\omega_{\mathbf{I}_k}(\mathbf{u}_k) + \widehat{\sigma}_{A,B} \cdot \omega_{\mathbf{I}_k}(\mathbf{u}_k)$ has no poles at $u_A = u_B$, thus $\widehat{\psi}_{\mathbf{I}_k}^{(L)}(\mathbf{u}_k; \mathbf{m}_L)$ and $\widehat{\mathcal{Z}}_k(\mathbf{u}_k; \mathbf{m}_L)$ are regular at $u_a = u_b$, $a, b = 1, \dots, L$, and polynomials of degree $L - 1$ in each u_a . \square

Lemma A.2. *One can decouple the vector multiplet scalars by*

$$(A.1) \quad \widehat{\mathcal{Z}}_k(\mathbf{u}_k; \mathbf{m}_L) = \frac{1}{L - k} \lim_{u_{k+1} \rightarrow \infty} u_{k+1}^{1-L} \widehat{\mathcal{Z}}_{k+1}(\mathbf{u}_{k+1}; \mathbf{m}_L),$$

and further,

$$(A.2) \quad \widehat{\mathcal{Z}}_k(\mathbf{u}_k; \mathbf{m}_L) = \frac{1}{(L - k)!} \lim_{u_{k+1}, \dots, u_L \rightarrow \infty} \left(\prod_{a=k+1}^L u_a^{1-L} \right) \widehat{\mathcal{Z}}_L(\mathbf{u}_L; \mathbf{m}_L)$$

Proof. The orbifold defect $\widehat{\psi}_{\mathbf{I}_k}^{(L)}(\mathbf{u}_k; \mathbf{m}_L)$ in (4.8) consists of $k!$ terms, and combining with the summation in (4.11), $\widehat{\mathcal{Z}}_k(\mathbf{u}_k; \mathbf{m}_L)$ contains $k! \times \binom{L}{k} = L!/(L-k)!$ terms in the summand. Comparing the summands on the both sides of (A.1), we find that the leading factor of $\widehat{\mathcal{Z}}_{k+1}(\mathbf{u}_{k+1}; \mathbf{m}_L)$ at $u_{k+1} \rightarrow \infty$ gives $(L - k) u_{k+1}^{L-1} \widehat{\mathcal{Z}}_k(\mathbf{u}_k; \mathbf{m}_L)$, and Equations (A.1) and (A.2) are obtained. \square

Equation (A.2) states that by decoupling the vector multiplet scalars u_a , $a = k + 1, \dots, L$, from $\widehat{\mathcal{Z}}_L(\mathbf{u}_L; \mathbf{m}_L) = \widehat{\psi}_{\mathbf{I}_L}^{(L)}(\mathbf{u}_L; \mathbf{m}_L)$, one obtains $\widehat{\mathcal{Z}}_k(\mathbf{u}_k; \mathbf{m}_L)$. For $\widehat{\mathcal{Z}}_L(\mathbf{u}_L; \mathbf{m}_L)$, we have the following proposition.

Proposition A.3. *The partition function $\widehat{\mathcal{Z}}_L(\mathbf{u}_L; \mathbf{m}_L)$ satisfies the same four conditions that define the $\mathfrak{su}(2)$ DWPF in [27]. Namely, $\widehat{\mathcal{Z}}_L(\mathbf{u}_L; \mathbf{m}_L)$*

1. *satisfies the initial condition $\widehat{\mathcal{Z}}_1(u; m) = 1$,*
2. *it is a polynomial of degree $L - 1$ in each u_a ,*
3. *it is invariant under any permutations of m_i 's, and*
4. *it satisfies the following recursion relation in L ,*

$$(A.3) \quad \widehat{\mathcal{Z}}_L(\mathbf{u}_L; \mathbf{m}_L) \Big|_{u_L = m_L - \frac{\gamma}{2}} = \prod_{a=1}^{L-1} \left(m_L - m_a - \gamma \right) \left(u_a - m_L - \frac{\gamma}{2} \right) \cdot \widehat{\mathcal{Z}}_{L-1}(\mathbf{u}_{L-1}; \mathbf{m}_{L-1})$$

Proof. Condition **1** follows from the definition of $\widehat{\mathcal{Z}}_L(\mathbf{u}_L; \mathbf{m}_L)$, and Condition **2** follows from Lemma A.1. To prove Condition **3**, it is sufficient to show that $\omega_{\mathbf{I}_L}(\mathbf{u}_L) + \widehat{\sigma}_{A,A+1} \cdot \omega_{\mathbf{I}_L}(\mathbf{u}_L)$, in $\widehat{\mathcal{Z}}_L(\mathbf{u}_L; \mathbf{m}_L)$, is invariant under the permutation of m_A and m_{A+1} , where $\omega_{\mathbf{I}_L}(\mathbf{u}_L) = \omega_{\mathbf{I}_L}^{(L)}(\mathbf{u}_L; \mathbf{m}_L)$ is defined in (4.9). The point is that, once this is shown, then by symmetrizing u_A , u_{A+1} , and u_{A+2} in $\omega_{\mathbf{I}_L}(\mathbf{u}_L)$, the symmetrized function becomes invariant under permuting m_A , m_{A+1} , and m_{A+2} . In $\omega_{\mathbf{I}_L}(\mathbf{u}_L)$, the factor that contains u_A and u_{A+1} is

$$(A.4) \quad \prod_{a=A,A+1}^L \left(\prod_{i=1}^{a-1} \left(u_a - m_i - \frac{\gamma}{2} \right) \cdot \prod_{i=a+1}^L \left(u_a - m_i + \frac{\gamma}{2} \right) \right) \cdot \frac{u_{A,A+1} - \gamma}{u_{A,A+1}} \\ \times \prod_{a=1}^{A-1} \frac{\left(u_{a,A} - \gamma \right) \left(u_{a,A+1} - \gamma \right)}{u_{a,A} u_{a,A+1}} \cdot \prod_{a=A+2}^L \frac{\left(u_{A,a} - \gamma \right) \left(u_{A+1,a} - \gamma \right)}{u_{A,a} u_{A+1,a}}$$

Because the factor that contains m_A and m_{A+1} , but does not contain u_A and u_{A+1} ,

$$(A.5) \quad \prod_{i=A,A+1}^L \left(\prod_{a=A+2}^L \left(u_a - m_i - \frac{\gamma}{2} \right) \cdot \prod_{i=1}^{A-1} \left(u_a - m_i + \frac{\gamma}{2} \right) \right),$$

is manifestly symmetric under the exchange of m_A and m_{A+1} , in $\omega_{\mathbf{I}_L}(\mathbf{u}_L) + \widehat{\sigma}_{A,A+1} \cdot \omega_{\mathbf{I}_L}(\mathbf{u}_L)$, it is sufficient to consider the following factor in (A.4)

$$(A.6) \quad \left(u_{A+1} - m_A - \frac{\gamma}{2} \right) \left(u_A - m_{A+1} + \frac{\gamma}{2} \right) \frac{u_{A,A+1} - \gamma}{u_{A,A+1}} \\ + \left(u_A - m_A - \frac{\gamma}{2} \right) \left(u_{A+1} - m_{A+1} + \frac{\gamma}{2} \right) \frac{u_{A,A+1} + \gamma}{u_{A,A+1}} \\ = - \left(m_A + m_{A+1} \right) \left(u_A + u_{A+1} \right) + 2 \left(m_A m_{A+1} + u_A u_{A+1} \right) + \frac{\gamma^2}{2}$$

Since this factor is symmetric under permuting m_A and m_{A+1} , Condition **3** is proved. To prove Condition **4**, we assign $u_L = m_L - \frac{\gamma}{2}$ in $\widehat{\mathcal{Z}}_L(\mathbf{u}_L; \mathbf{m}_L)$, the non-zero terms only come from $\text{Sym}_{\mathbf{u}_{L-1}} \omega_{\mathbf{I}_L}(\mathbf{u}_L)$, and by

$$(A.7) \quad \widehat{\mathcal{Z}}_L(\mathbf{u}_L; \mathbf{m}_L) \Big|_{u_L = m_L - \frac{\gamma}{2}} = \\ \prod_{a=1}^{L-1} \left(u_L - m_a - \frac{\gamma}{2} \right) \left(u_a - m_L + \frac{\gamma}{2} \right) \frac{u_{a,L} - \gamma}{u_{a,L}} \Big|_{u_L = m_L - \frac{\gamma}{2}} \times \widehat{\mathcal{Z}}_{L-1}(\mathbf{u}_{L-1}; \mathbf{m}_{L-1}),$$

the recursion relation (A.3) is obtained. \square

By induction in L , any function which satisfies the four conditions in Proposition A.3 is uniquely determined⁹, and the partition function $\widehat{\mathcal{Z}}_L(\mathbf{u}_L; \mathbf{m}_L)$ agrees with Izergin's determinant expression for the $\mathfrak{su}(2)$ DWPF [28] (see [31] for a review), which satisfies the same four conditions, as well as Kostov's determinant expression [18, 19], which is equivalent to Izergin's.

⁹ Condition **1** gives the initial condition of the recursion, Condition **2** implies that the solution of the recursion is uniquely determined by L conditions on the values of any of the variables u_a , and Conditions **3** and **4** give the necessary L conditions on the values of the variable u_L .

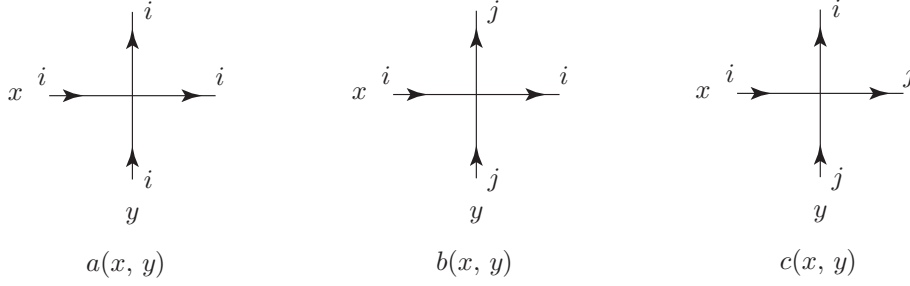


FIGURE 11. The non-zero vertex (Boltzmann) weights $w_v(x, y)$ (whose values are given in (B.4) in the case of the rational models, and in (B.5) in the case of the trigonometric models) that can be assigned to a vertex v . The arrows indicate the directions of rapidity and inhomogeneity parameter flows, and the integers $i, j = 1, \dots, M+1$, $i \neq j$, are the state variables, or colours assigned to the bonds.

Proposition A.4. *The partition function $\widehat{\mathcal{Z}}_L(\mathbf{u}_L; \mathbf{m}_L)$ is an Izergin determinant [28]*

$$(A.8) \quad \widehat{\mathcal{Z}}_L(\mathbf{u}_L; \mathbf{m}_L) = \frac{\prod_{a,b=1}^L \left(u_a - m_b - \frac{\gamma}{2} \right) \left(u_a - m_b + \frac{\gamma}{2} \right)}{\prod_{a < b}^L u_{b,a} m_{a,b}} \times \det \left(\frac{1}{\left(u_a - m_b - \frac{\gamma}{2} \right) \left(u_a - m_b + \frac{\gamma}{2} \right)} \right)_{a,b=1,\dots,L},$$

or equivalently, a Kostov determinant [18, 19],

$$(A.9) \quad \widehat{\mathcal{Z}}_L(\mathbf{u}_L; \mathbf{m}_L) = \frac{\prod_{a,b=1}^L \left(u_a - m_b + \frac{\gamma}{2} \right)}{\prod_{a < b}^L u_{b,a}} \times \det \left(u_a^{b-1} \prod_{i=1}^L \frac{u_a - m_i - \frac{\gamma}{2}}{u_a - m_i + \frac{\gamma}{2}} - (u_a - \gamma)^{b-1} \right)_{a,b=1,\dots,L},$$

which is an $\mathfrak{su}(2)$ DWPF, where $m_{a,b} = m_a - m_b$.

Proof of Proposition 4.5. Taking the decoupling limit (A.2) in Proposition A.4, Proposition 4.5 is proved. \square

APPENDIX B. THE $\mathfrak{su}(M+1)$ VERTEX MODEL ASSOCIATED WITH THE A_M QUIVER

We describe the lattice configurations that represent the partition functions of the rational $\mathfrak{su}(M+1)$ vertex model that corresponds to the $\mathfrak{su}(M+1)$ XXX spin-chain with spins in the fundamental representation.

B.1. Notation.

$$(B.1) \quad \begin{aligned} \mathbf{x}_k^M &= \{\mathbf{x}_{k_1}^{(1)}, \dots, \mathbf{x}_{k_M}^{(M)}\}, & \mathbf{x}_{k_p}^{(p)} &= \{x_1^{(p)}, \dots, x_{k_p}^{(p)}\}, \\ \mathbf{y}_L^M &= \{\mathbf{y}_{L_1}^{(1)}, \dots, \mathbf{y}_{L_M}^{(M)}\}, & \mathbf{y}_{L_p}^{(p)} &= \{y_1^{(p)}, \dots, y_{L_p}^{(p)}\}, \quad p = 1, \dots, M, \end{aligned}$$

where $x_a^{(p)}$ and $y_a^{(p)}$ are the rapidities and inhomogeneities, respectively. The translation of the lattice parameters to the gauge theory parameters in Table 1 is

$$(B.2) \quad x_a^{(p)} = u_a^{(p)} - \left(\frac{M-p+1}{2} \right) \gamma, \quad y_i^{(p)} = m_i^{(p)} - \left(\frac{M-p}{2} \right) \gamma, \quad \gamma = 1$$

B.2. The vertex model. A square lattice representation of the rational $\mathfrak{su}(M+1)$ vertex model consists of horizontal lines that carry x -variables that flow from right to left, and vertical lines that carry y -variables that flow from bottom to top. The horizontal lines and the vertical lines intersect in vertices, and each vertex is connected to 4 line-segments that we call *bonds*. An internal bond is connected to two vertices and a boundary bond is connected to a single vertex. Each bond carries an arrow that indicates direction of the variable flow along it¹⁰. Further, each bond carries a colour $i \in \{1, \dots, M+1\}$, and colour is conserved¹¹, that is, if the colours on the bonds with incoming variable flows are i and j , the colours on the bonds with outgoing variable flows are k and l , then

$$(B.3) \quad i + j = k + l$$

Given colour conservation (B.3), there are three types of vertices, type-*a*, type-*b* and type-*c*, as in Figure 11, with vertex weights that depend (at most) on difference of variables

$$(B.4) \quad a(x, y) = x - y + 1, \quad b(x, y) = x - y, \quad c(x, y) = 1$$

Remark B.1. The vertex weights in the trigonometric $\mathfrak{su}(M+1)$ vertex model, which corresponds to the $\mathfrak{su}(M+1)$ XXZ spin-chain with spins in the fundamental representation, are

$$(B.5) \quad a(x, y) = [x - y + 1], \quad b(x, y) = [x - y], \quad c(x, y) = [1],$$

where $[x] = 2 \sinh(x/2)$.

We associate lattice configurations to the A_M linear quiver in Figure 1, where $k_p \leq L_p + k_{p+1}$, $k_M \leq L_M$, $p = 1, \dots, M-1$, as follows. For the first node with $U(k_1)$ gauge group, we associate one of the lattice configurations in Figure 12.

¹⁰ This is necessary to make the vertex type and weight, see below, of the different vertices unambiguous.

¹¹ This is the case in rational and trigonometric vertex $\mathfrak{su}(M+1)$ models, with three types of vertices, but not in elliptic vertex models which has a fourth type of vertices that conserve colour only modulo $M+1$.

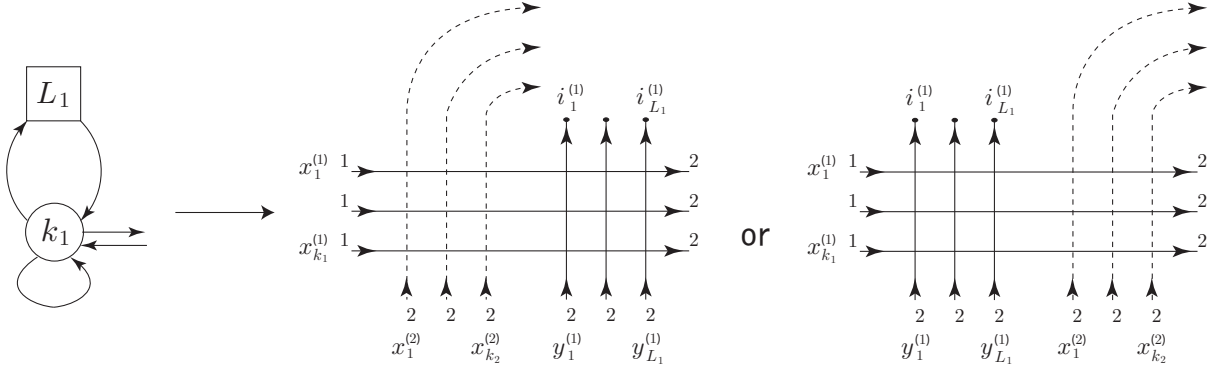


FIGURE 12. Two possible lattice configurations that can be associated with the first quiver node.

All bonds on the left boundary are assigned the (fixed and same) colour 1, all bonds on the right and lower boundaries are assigned the (fixed and same) colour 2, and the L_1 bonds on the top boundary are assigned (fixed but varying) colours $i_\ell^{(1)} \in \{1, 2\}$, $\ell = 1, \dots, L_1$. Each dashed line that carries a rapidity variable $x_a^{(2)}$ is connected with another dashed line that carries a rapidity variable $x_a^{(2)}$ associated with the second quiver node. For the p -th quiver node with a $U(k_p)$ gauge group, $p = 2, \dots, M-1$, we associate one of the lattice configurations in Figure 13, where, each dashed line that carries a rapidity $x_a^{(p)}$ is connected with another dashed line that carries a rapidity variable $x_a^{(p)}$.

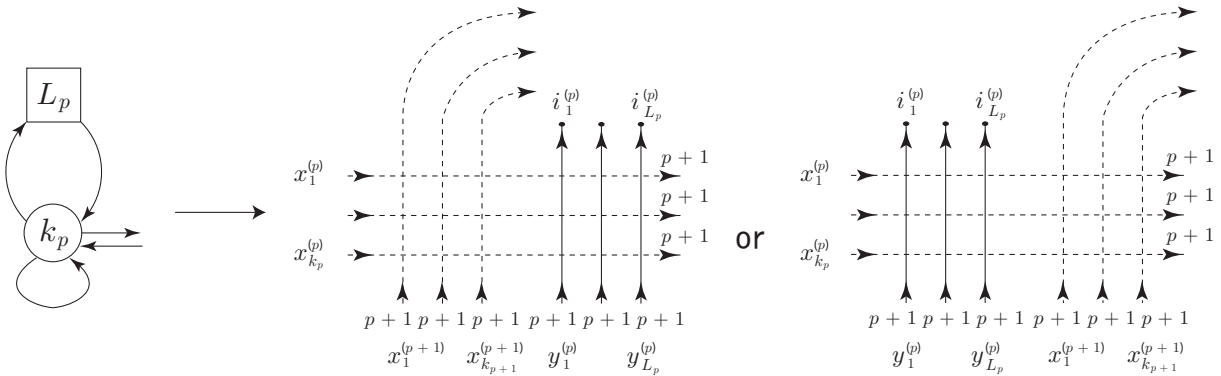
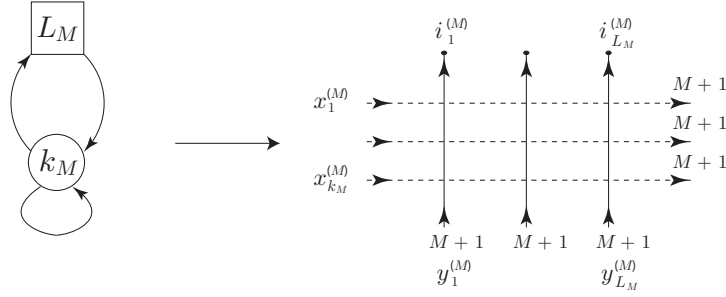


FIGURE 13. Two possible lattice configurations that can be associated with the p -th quiver node, where $p = 2, \dots, M-1$.

All bonds on the right boundary and on the lower boundary are assigned the (fixed and same) colour $p+1$, the L_p bonds on the top boundary are assigned (fixed but varying) colours $i_\ell^{(L_p)} \in \{1, \dots, p+1\}$, $\ell = 1, \dots, L_p$, and we label the above left (resp. right) associated lattice configuration by $s_p = 1$ (resp. $s_p = 2$). For the M -th quiver node with $U(k_M)$ gauge group, we associate the unique lattice configuration in Figure 14.

FIGURE 14. A lattice configuration associated with the M -th node.

The bonds on the right and lower boundaries are assigned the (fixed and same) colour $M+1$, and the L_M bonds on the top boundary are assigned (fixed but varying) colours $i_\ell^{(L_M)} \in \{1, \dots, M+1\}$, $\ell = 1, \dots, L_M$. From colour conservation,

$$(B.6) \quad \sum_{p=1}^M \#_1 \left(\mathbf{i}_{L_p}^{(p)} \right) = k_1, \quad \sum_{p=q-1}^M \#_q \left(\mathbf{i}_{L_p}^{(p)} \right) = k_q - k_{q-1}, \quad q = 2, \dots, M,$$

$$\#_{M+1} \left(\mathbf{i}_{L_M}^{(M)} \right) = L_M - k_M,$$

where $\#_q(\mathbf{i}_{L_p}^{(p)})$ is the number of colours q in the set $\mathbf{i}_{L_p}^{(p)} = \{i_1^{(p)}, \dots, i_{L_p}^{(p)}\}$. Examples of $\mathfrak{su}(2)$ and $\mathfrak{su}(3)$ lattice configurations are in Figures 3 and 7, respectively.

Definition B.2. *The partition function for the rational/trigonometric $\mathfrak{su}(M+1)$ lattice configuration associated with the A_M linear quiver in Figure 1 is defined by*

$$(B.7) \quad \widehat{\psi}_{\mathbf{L}, \mathbf{i}_{\mathbf{L}}^M}^{(\mathbf{S}|\mathbf{L})} \left(\mathbf{x}_{\mathbf{k}}^M; \mathbf{y}_{\mathbf{L}}^M \right) = \sum_{\sigma|_{\mathbf{i}_{\mathbf{L}}^M}} \prod_{v \in \mathbf{v}|\sigma} w_v \left(\mathbf{x}_1^{(v)}, \mathbf{x}_2^{(v)} \right),$$

where $\mathbf{i}_{\mathbf{L}}^M = \{\mathbf{i}_{L_1}^{(1)}, \dots, \mathbf{i}_{L_M}^{(M)}\}$ and $\mathbf{S} = \{s_1, \dots, s_{M-1}\}$, $s_p \in \{1, 2\}$. $\sigma|_{\mathbf{i}_{\mathbf{L}}^M}$ is a lattice configuration with fixed boundary colours $\mathbf{i}_{\mathbf{L}}^M$, and $\mathbf{v}|\sigma$ is the set of all vertices on the lattice with the lattice configuration σ . $w_v(\mathbf{x}_1^{(v)}, \mathbf{x}_2^{(v)})$ is the vertex weight on the vertex v defined in Figure 11, where $\mathbf{x}_1^{(v)}$ and $\mathbf{x}_2^{(v)}$ are the corresponding variables.

REFERENCES

- [1] N Nekrasov, *Bethe States As Defects In Gauge Theories*, (2013) http://scgp.stonybrook.edu/video_portal/video.php?id=1775
- [2] N Nekrasov, *Bethe wavefunctions from gauged linear sigma models via Bethe/Gauge correspondence*, (2014) http://scgp.stonybrook.edu/video_portal/video.php?id=1360
- [3] M Bullimore, H C Kim and T Lukowski, *Expanding the Bethe/Gauge Dictionary*, Journal of High Energy Physics **1711**, 055 (2017), [arXiv:1708.00445](https://arxiv.org/abs/1708.00445) [hep-th]
- [4] N A Nekrasov and S L Shatashvili, *Supersymmetric vacua and Bethe ansatz*, Nuclear Physics Proceedings Supplement **192-193**, 91 (2009), [arXiv:0901.4744](https://arxiv.org/abs/0901.4744) [hep-th]
- [5] N A Nekrasov and S L Shatashvili, *Quantum integrability and supersymmetric vacua*, Progress Theoretical Physics Supplement **177**, 105 (2009), [arXiv:0901.4748](https://arxiv.org/abs/0901.4748) [hep-th]

- [6] M Gaudin, *The Bethe wavefunction*, translated from French by J S Caux, Cambridge University Press, 2014, ISBN-10: 1107045851
- [7] F H L Essler, H Frahm, F Göhmann, A Klumper, and V E Korepin, *The one-dimensional Hubbard model*, Cambridge University Press, 2005, ISBN-10: 0521802628
- [8] C Closset, S Cremonesi and D S Park, *The equivariant A-twist and gauged linear sigma models on the two-sphere*, Journal of High Energy Physics **1506**, 076 (2015), arXiv:1504.06308 [hep-th]
- [9] F Benini and A Zaffaroni, *A topologically twisted index for three-dimensional supersymmetric theories*, Journal of High Energy Physics **1507**, 127 (2015), arXiv:1504.03698 [hep-th]
- [10] E Witten, *Phases of $N = 2$ theories in two-dimensions*, Nuclear Physics **B 403**, 159 (1993), hep-th/9301042
- [11] D R Morrison and M R Plesser, *Summing the instantons: Quantum cohomology and mirror symmetry in toric varieties*, Nuclear Physics **B 440**, 279 (1995), hep-th/9412236
- [12] L C Jeffrey and F C Kirwan, *Localization for nonabelian group actions*, Topology **34**, no. 2, 291-327 (1995), arXiv:alg-geom/9307001
- [13] M Brion and M Vergne, *Arrangements of hyperplanes I: Rational functions and Jeffrey-Kirwan residue*, Annales Scientifiques de l'École Normale Supérieure (4) **32**, 715-741 (1999), arXiv:math/9903178 [math.DG]
- [14] A Szenes and M Vergne, *Toric reduction and a conjecture of Batyrev and Materov*, Inventiones mathematicae **158**, no. 3, 453-495 (2004), arXiv:math/0306311 [math.AT]
- [15] F Benini, R Eager, K Hori and Y Tachikawa, *Elliptic Genera of 2d $\mathcal{N} = 2$ Gauge Theories*, Communications in Mathematical Physics **333**, no. 3, 1241 (2015), arXiv:1308.4896 [hep-th]
- [16] D Gaiotto and P Koroteev, *On Three Dimensional Quiver Gauge Theories and Integrability*, Journal of High Energy Physics **1305**, 126 (2013), arXiv:1304.0779 [hep-th]
- [17] O Foda and M Wheeler, *Partial domain wall partition functions*, Journal of High Energy Physics **1207**, 186 (2012), arXiv:1205.4400 [math-ph]
- [18] I Kostov, *Classical Limit of the Three-Point Function of $\mathcal{N} = 4$ Supersymmetric Yang-Mills Theory from Integrability*, Physical Review Letters **108**, 261604 (2012), arXiv:1203.6180 [hep-th]
- [19] I Kostov, *Three-point function of semiclassical states at weak coupling*, Journal of Physics **A 45**, 494018 (2012), arXiv:1205.4412 [hep-th]
- [20] M Mestyán, B Bertini, L Piroli and P Calabrese, *Exact solution for the quench dynamics of a nested integrable system*, Journal of Statistical Mechanics **1708**, no. 8, 083103 (2017), arXiv:1705.00851 [cond-mat.stat-mech]
- [21] D Shenfeld, *Abelianization of Stable Envelopes in Symplectic Resolutions*, PhD thesis, Princeton, 2013
- [22] D Maulik and A Okounkov, *Quantum Groups and Quantum Cohomology*, arXiv:1211.1287 [math.AG]
- [23] R Rimanyi, V Tarasov and A Varchenko, *Partial flag varieties, stable envelopes and weight functions*, Quantum Topology **6**, no. 2, 333-364 (2015), arXiv:1212.6240 [math.AG]
- [24] M Aganagic and A Okounkov, *Quasimap counts and Bethe eigenfunctions*, Moscow Mathematical Journal **17**, no. 4, 565 (2017), arXiv:1704.08746 [math-ph]
- [25] O Foda and M Wheeler, *Colour-independent partition functions in coloured vertex models*, Nuclear Physics **B 871**, 330 (2013), arXiv:1301.5158 [math-ph]
- [26] A Hanany and E Witten, *Type IIB superstrings, BPS monopoles, and three-dimensional gauge dynamics*, Nuclear Physics **B 492**, 152 (1997), hep-th/9611230
- [27] V E Korepin, *Calculation Of Norms Of Bethe Wave Functions*, Communications in Mathematical Physics **86**, 391 (1982)
- [28] A G Izergin, *Partition function of the six-vertex model in a finite volume*, Soviet Physics Doklady **32**, 878 (1987)
- [29] G Bonelli, A Sciarappa, A Tanzini and P Vasko, *Quantum Cohomology and Quantum Hydrodynamics from Supersymmetric Quiver Gauge Theories*, Journal of Geometry and Physics **109**, 3 (2016), arXiv:1505.07116 [hep-th]

- [30] G Bonelli, N Fasola and A Tanzini, *Defects, nested instantons and comet shaped quivers*, arXiv:1907.02771 [hep-th]
- [31] M A Wheeler, *Free fermions in classical and quantum integrable models*, PhD thesis, Melbourne, 2010, arXiv:1110.6703 [math-ph]

SCHOOL OF MATHEMATICS AND STATISTICS, UNIVERSITY OF MELBOURNE, ROYAL PARADE, PARKVILLE, VICTORIA 3010, AUSTRALIA

E-mail address: omar.foda@unimelb.edu.au, masahidemanabe@gmail.com